Molecular Psychiatry (2016) 00, 1–9

www.nature.com/mp

ORIGINAL ARTICLE

Heightened extended amygdala metabolism following threat characterizes the early phenotypic risk to develop anxiety-related psychopathology

AJ Shackman[1,2,3,12], AS Fox[4,12], JA Oler[5,6,7], SE Shelton[5], TR Oakes[8], RJ Davidson[5,6,9,10,11] and NH Kalin[5,6,7,11]

Children with an anxious temperament are prone to heightened shyness and behavioral inhibition (BI). When chronic and extreme, this anxious, inhibited phenotype is an important early-life risk factor for the development of anxiety disorders, depression and co-morbid substance abuse. Individuals with extreme anxious temperament often show persistent distress in the absence of immediate threat and this contextually inappropriate anxiety predicts future symptom development. Despite its clear clinical relevance, the neural circuitry governing the maladaptive persistence of anxiety remains unclear. Here, we used a well-established nonhuman primate model of childhood temperament and high-resolution ^{18}fluorodeoxyglucose positron emission tomography (FDG-PET) imaging to understand the neural systems governing persistent anxiety and to clarify their relevance to early-life phenotypic risk. We focused on BI, a core component of anxious temperament, because it affords the moment-by-moment temporal resolution needed to assess contextually appropriate and inappropriate anxiety. From a pool of 109 peri-adolescent rhesus monkeys, we formed groups characterized by high or low levels of BI, as indexed by freezing in response to an unfamiliar human intruder's profile. The high-BI group showed consistently elevated signs of anxiety and wariness across >2 years of assessments. At the time of brain imaging, 1.5 years after initial phenotyping, the high-BI group showed persistently elevated freezing during a 30-min 'recovery' period following an encounter with the intruder—more than an order of magnitude greater than the low-BI group—and this was associated with increased metabolism in the bed nucleus of the stria terminalis, a key component of the central extended amygdala. These observations provide a neurobiological framework for understanding the early phenotypic risk to develop anxiety-related psychopathology, for accelerating the development of improved interventions, and for understanding the origins of childhood temperament.

Molecular Psychiatry advance online publication, 30 August 2016; doi:10.1038/mp.2016.132

INTRODUCTION

When stable and extreme, anxious temperament is a prominent childhood risk factor for the development of anxiety disorders, depression and co-morbid substance abuse.[1,2] These disorders are common, debilitating and challenging to treat,[3] highlighting the need to develop a deeper understanding of the neural systems that support elevated levels of dispositional anxiety and confer increased risk for the development of anxiety-related psychopathology.

Children with an anxious temperament often show sustained levels of heightened shyness, neuroendocrine activity and behavioral inhibition (BI; for example, freezing) in response to novelty and potential threat.[4,5] Anxious temperament is a trait-like phenotype that is determined by a combination of heritable and non-heritable factors, evident early in life, decreased by the administration of anxiolytic agents and expressed similarly in children and young monkeys.[4–8]

Persistent distress in the absence of immediate danger is a key feature of temperamental anxiety.[9,10] Like adults,[11–13] children with extreme anxiety show potentiated defensive responses (for example, startle) and report increased distress during periods of explicit safety before and after the presentation of threat.[14–18] Contextually inappropriate anxiety in the laboratory prospectively predicts heightened anxiety and exaggerated avoidance in the real world.[19,20] Among adults with anxiety and depressive disorders, heightened 'spillover' and inertia of negative mood are common and predict the severity of clinical symptoms,[21,22] the onset of future episodes of psychopathology[23] and treatment response.[22]

Despite its clear clinical relevance, the neural circuitry governing the maladaptive persistence of anxiety in the minutes or hours following encounters with threat or other stressors remains poorly understood.[24] Recent work highlights the potential importance of the central extended amygdala, an anatomical concept encompassing the central (Ce) nucleus of the amygdala and the neighboring bed nucleus of the stria terminalis (BST). Mechanistic work in rodents indicates that the extended amygdala coordinates persistent defensive responses elicited by prolonged exposure to

[1]Department of Psychology, University of Maryland, College Park, MD, USA; [2]Neuroscience and Cognitive Science Program, University of Maryland, College Park, MD, USA; [3]Maryland Neuroimaging Center, University of Maryland, College Park, MD, USA; [4]Department of Psychology and California National Primate Research Center, University of California, Davis, CA, USA; [5]Department of Psychiatry, University of Wisconsin, Madison, WI, USA; [6]HealthEmotions Research Institute, University of Wisconsin, Madison, WI, USA; [7]Lane Neuroimaging Laboratory, University of Wisconsin, Madison, WI, USA; [8]inseRT MRI, Inc., Middleton, WI, USA; [9]Department of Psychology, University of Wisconsin, Madison, WI, USA; [10]Center for Investigating Healthy Minds, University of Wisconsin, Madison, WI, USA and [11]Waisman Laboratory for Brain Imaging and Behavior, University of Wisconsin, Madison, WI, USA. Correspondence: Dr NH Kalin, Department of Psychiatry, University of Wisconsin, 6001 Research Park Boulevard, Madison, Wisconsin 53719, USA.
E-mail: nkalin@wisc.edu
[12]These authors contributed equally to this work.
Received 31 October 2015; revised 19 May 2016; accepted 1 June 2016

uncertain threat cues (for example, cues paired with temporally unpredictable shock delivery) and diffusely threatening contexts (for example, elevated-plus maze, brightly lit open field).[11,24–27] Imaging studies in monkeys demonstrate that activity in the extended amygdala predicts individual differences in freezing and other components of anxious temperament.[28,29] Imaging studies in humans reveal increased activation in the dorsal amygdala in response to novel and potentially threatening faces among individuals with a childhood history of extreme BI.[5]

Here, we used a well-established nonhuman primate model of childhood anxiety and high-resolution ^{18}fluorodeoxyglucose (^{18}FDG) positron emission tomography (PET) imaging to establish the contribution of the primate-extended amygdala to persistently enhanced, context-inappropriate freezing during the 'recovery' period following an encounter with potential threat. We focused on freezing, a core component of the BI phenotype in children[4,30] and the broader anxious temperament phenotype in monkeys,[5–7] because it affords the moment-by-moment temporal resolution needed to assess contextually appropriate and inappropriate anxiety. Young rhesus monkeys are ideal for understanding the neurobiology of extreme early-life anxiety. Reflecting the two species comparatively recent evolutionary divergence, the brains of rhesus monkeys and human children are genetically, anatomically and functionally similar.[31,32] This is important, given known anatomical differences in the extended amygdala between rodents and primates.[33,34] Homologous neurobiological substrates endow monkeys and humans with a shared repertoire of complex cognitive and socio-emotional behaviors, and a common set of defensive responses to potential danger.[5,7]

Adopting the longitudinal, extreme groups strategy widely used to identify children at greatest risk,[1,4] we phenotyped 109 peri-adolescent rhesus monkeys (M (s.d.) = 2.19 years (0.50); range = 1.45–3.42 years) on two occasions 1 week apart and formed groups with stable high ($n = 11$; top quartile) or stable low levels of BI ($n = 12$; bottom quartile; Figures 1a and b). Here, the BI phenotype was quantified by measuring freezing in response to an unfamiliar human intruder's profile (that is, the 'No Eye Contact' condition of the Human Intruder Paradigm[35]), paralleling methods used in children.[7] To further assess the long-term stability and generality of the monkey BI phenotype, snake anxiety was assessed ~2 years after the initial phenotyping (Figure 1c).

A key advantage of the nonhuman primate model is that it permits concurrent measures of regional brain metabolism and naturalistic defensive responses. Here, the extreme BI groups were imaged on two occasions, >1.5 years after the initial phenotyping (Figure 1d). In the threat condition, subjects were placed in a testing cage and exposed to the human intruder's profile for 30 min. Next, they received an injection of the radiotracer ^{18}FDG and were returned to the testing cage, where they were allowed to recover from the threat encounter for 30 min. At the end of this 'recovery' period, subjects were anesthetized and positioned in the PET scanner. The control condition differed only in the absence of threat exposure during the initial 30-min. Comparison of the physically identical 'recovery' phases of the threat and control conditions enabled us to assess persistent group differences in freezing and accompanying brain activity. In contrast to conventional functional magnetic resonance imaging (fMRI) techniques, FDG-PET, which provides a measure of regional brain metabolism integrated over the 30-min 'recovery' period, is uniquely well suited for assessing sustained neural responses.[36] Establishing the neural systems that support persistent, contextually inappropriate anxiety is important for understanding the mechanisms that contribute to the development and maintenance of psychopathology, for guiding the development of improved prevention and treatment strategies, and for understanding the neural bases of childhood temperament.

MATERIALS AND METHODS

Subjects

Peri-adolescent rhesus monkeys (*Macaca mulatta*; $n = 109$; 63.3% female; M (s.d.) = 2.19 years (0.50); range = 1.45–3.42 years) were tested as part of a larger program of research to understand the mechanisms underlying early-life anxiety.[6,37–39] Data were collected between September 2004 and November 2006. Hypothesis testing focused on data obtained from 23 animals selected on the basis of stable and extreme levels of freezing (high-BI: $n = 11$; low-BI: $n = 12$; Table 1). We focused on freezing because, in contrast to other components of anxious temperament phenotype (for example, cortisol), it affords the temporal resolution needed to dissociate recovery from the acute impact of exposure to the intruder's profile (cf. Figure 1d). The procedures used for forming extreme groups are detailed below. In contrast to *post hoc* dichotomization, the use of extreme groups is scientifically and statistically appropriate, given our focus on stable and extreme levels of BI.[40] Prior work by our group using similar extreme groups designs indicates adequate power to detect large mean differences with 11–12 animals per group (for example, 92.9% power to detect $d = 1.5$ using two-tailed $\alpha = 0.05$).[41,42] All procedures were in accord with guidelines established by the local Institutional Animal Care and Use Committee.

General procedures

All techniques have been described in detail in prior publications by our group.[6,37–39] Experimental personnel were blind to group status at the time of data collection. For additional details, see the Supplementary Methods.

Formation of groups with stable and extreme BI

Research in children indicates that individuals who consistently express high levels of BI (for example, more persistent freezing, fewer vocalizations) across repeated assessments are at the greatest risk for the development of psychopathology.[1,43] Accordingly, groups with stable, extreme levels of the BI phenotype were formed by organizing animals into quartiles based on $\log_{10}$-transformed freezing during exposure to the human intruder's profile for the first, second and mean of the two phenotyping sessions (Figure 1a). Individual differences in intruder-elicited freezing were continuously distributed without obvious gaps or discontinuities (Supplementary Figure S1), consistent with prior work by our group.[28] Subjects who remained in the same quartile across the three metrics were deemed stable. Age- and sex-matched groups were formed using the most extreme individuals with stable phenotypes. During the initial phenotyping sessions, freezing was also assessed in the absence of potential threat (that is, the 'Alone' condition of the Human Intruder Paradigm;[7,35] Figure 1a). The Alone condition was always administered first to circumvent carry-over from the higher-intensity intruder challenge

Snake anxiety

To clarify the stability and generality of the BI phenotype, snake anxiety was assessed using standard techniques[42] (Supplementary Methods) ~2 years after initial phenotyping (Figure 1c). Subjects were pre-trained to retrieve preferred foods. During the assessment, foods were placed on top of a transparent enclosure containing a live snake, comparison stimuli (that is, artificial snake, roll of tape), or nothing (6 trials/condition; order counterbalanced). Because many subjects refused to respond in the presence of the live snake (55% and 17% of the high- and low-BI groups, respectively), anxiety was assessed using the total number of non-responses (square-root transformed), circumventing the need to omit subjects with incomplete response time data and maximizing statistical power.

FDG-PET and MRI data acquisition

Brain FDG metabolism was measured on two occasions (that is, the threat and control conditions depicted in Figure 1d) ~1.5 years after the phenotyping sessions (M (s.d.) interval = 1.62 (0.06) years; Table 1). The order of the two FDG-PET sessions was pseudo-randomized across subjects and balanced across groups. Imaging sessions occurred within 28 days of one another ($M = 2.20$ weeks, s.d. = 1.10). Subjects were acclimated to the imaging procedures before the first FDG-PET session (Supplementary Methods). FDG-PET reflects the amount of regional FDG uptake and metabolism between the injection and PET scan, with majority of uptake occurring in the first 30 min. Anatomical scans were collected using a GE Signa 3 T MRI

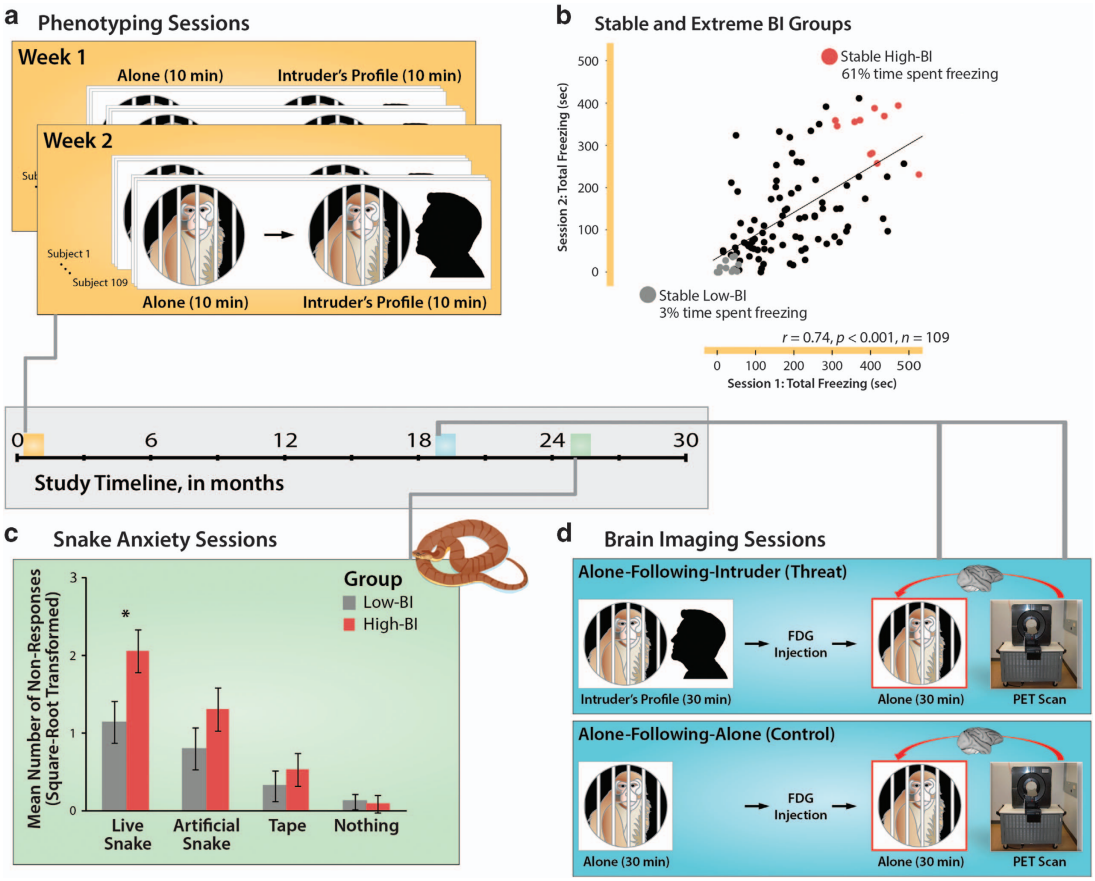

Figure 1. Overview of longitudinal phenotyping and brain imaging procedures. The horizontal axis at the center of the figure depicts the relative timing of the longitudinal assessments. (**a**) Phenotyping sessions. Individual differences in freezing elicited by diffuse threat (i.e. 10 min exposure to the testing cage) and potential threat (that is, 10 min exposure to the human intruder's profile) were assessed in 109 monkeys twice, one week apart using the 'Alone' and 'No Eye Contact' conditions of the Human Intruder Paradigm.[7,35] The Alone condition was always administered first to circumvent carry-over from the higher-intensity intruder challenge. (**b**) Formation of stable and extreme BI groups. Groups were formed from individuals who consistently showed extreme freezing in response to the intruder's profile across the two phenotyping sessions. Age- and sex-matched high-BI and low-BI groups are depicted in red and gray, respectively. For illustrative purposes, the *x*- and *y*-axes indicate the total number of seconds spent freezing during the 10-min intruder challenges. Inferential statistics employed $\log_{10}$-transformed freezing. (**c**) Snake anxiety sessions. More than 2 years after initial assessment, subjects were trained to retrieve highly preferred foods in the Wisconsin General Testing Apparatus. During the snake anxiety assessment, foods were placed on top of a clear enclosure containing a live snake, an artificial snake, a roll of tape or nothing. As shown in the bar plot, the stable high-BI group shows significantly greater passive avoidance in the presence of the live snake (group × stimulus, $P < 0.05$). Asterisk indicates significant pairwise group difference. Error bars depict s.e. (**d**) Brain imaging sessions. Approximately 1.5 years after the initial assessment, subjects were scanned. FDG-PET (^{18}fluorodeoxyglucose positron emission tomography) scanning was conducted in two sessions (order pseudo-randomized). Subjects were acclimated to behavioral testing procedures for 5 days before the first scanning session. In the threat condition (upper blue panel), subjects were placed in a testing cage and exposed to the human intruder's profile for 30 min. To minimize habituation, the intruder presented his profile for 10 min, exited the testing environment, returned after 5 min, presented his profile for 5 min, exited for 5 min and then presented for a final 5 min. At the end of the 30-min challenge, subjects received an injection of the radiotracer ^{18}FDG and were returned to the testing cage. At the end of this 30-min 'recovery' period, subjects were anesthetized and positioned in the high-resolution, small-bore PET scanner. The control condition (lower blue panel) differed only in the absence of threat exposure during the initial 30-min. Comparison of the physically identical 'recovery' periods of the threat and control conditions (red boxes) enabled us to assess group differences in regional brain activity following the intruder encounter. Portions of this figure were adapted with permission from refs. 83,84. BI, behavioral inhibition.

scanner, standard quadrature coil and a 3D T1-weighted, inversion-recovery, gradient-echo prescription (TI/TR/TE/Flip/NEX/FOV/Matrix/Bandwidth/Slices/Gap: 600 ms/8.648 ms/1.888 ms/10°/2/140 mm/256 × 224/61.0547 kHz/128/-0.5 mm; reconstructed to 0.2734 × 0.2734 × 0.5 mm). Brain activity during the first half of the session (Figure 1d), before FDG administration, was not measured.

Brain imaging data processing pipeline

As detailed in the Supplementary Methods, T1-weighted anatomical images and FDG-PET data were normalized to a study-specific rhesus template (0.625 mm^3) using standard techniques. Anatomical images were segmented using FAST (http://www.fmrib.ox.ac.uk/fsl/fast4). PET and gray matter probability maps were smoothed 4 mm.

Hypothesis testing strategy

Brain and behavioral data were carefully inspected to ensure that inferential test assumptions were adequately satisfied. As detailed in the Supplementary Methods, we used a series of voxelwise general linear models to identify regions (i) where the group (high-BI, low-BI) × condition (Alone-following-Intruder, Alone-following-Alone) interaction was significant and (ii) where the high-BI group showed significantly more metabolism than the low-BI group during the critical 30-min 'recovery' period following the threat encounter (Alone-following-Intruder). Given

Table 1. Descriptive statistics for the extreme BI groups

Age (years)[a]	*High BI*[b]		*Low BI*[c]	
	M	*s.d.*	*M*	*s.d.*
First screening session	2.31	0.57	2.14	0.53
First FDG-PET session	3.94	0.60	3.76	0.56
Second FDG-PET session	3.99	0.60	3.80	0.57
Snake anxiety assessment	4.45	0.62	4.26	0.56

Abbreviations: BI, behavioral inhibition; FDG-PET, ^{18}fluorodeoxyglucose positron emission tomography. [a]The groups did not differ in sex or age, $Ps > 0.44$. [b]Consisted of 8 females and 3 males. [c]Consisted of 9 females and 3 males.

our *a priori* focus on the contributions of the extended amygdala, each test was thresholded at $P < 0.05$, corrected for a region of interest (ROI) encompassing the amygdala, BST and substantia innominata. To identify regions satisfying both of these key criteria, thresholded maps were combined using a minimum conjunction (logical AND),[44] as in prior work by our group.[28] To provide additional information about specificity, clusters lying outside of the ROI that survived the small-volume threshold are depicted visually and detailed in Supplementary Tables (that is, they were not masked). On an exploratory basis, we also assessed whether they survived a whole-brain, cluster-extent threshold. The code and scripts used to conduct these analyses is available upon request.

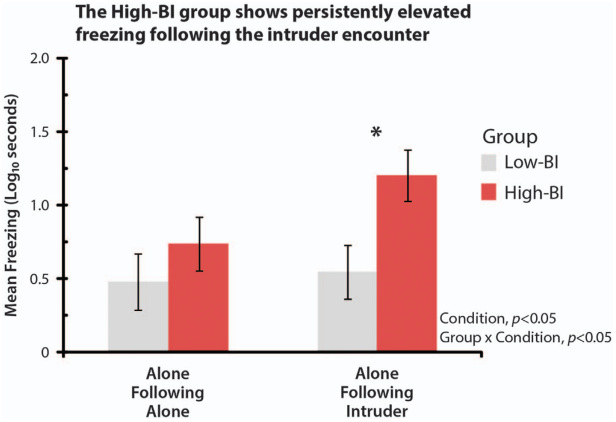

Figure 2. The stable high-BI (behavioral inhibition) group shows persistently elevated freezing during the 'recovery' period following the intruder encounter (1.5 years later). See Figure 1d for an overview of the paradigm. The groups did not significantly differ in the Alone-following-Alone control condition ($P = 0.35$). The high-BI group froze longer following the encounter (Alone-following-Intruder) compared with the control condition (Alone-following-Alone; $F(1,21) = 12.04$, $P = 0.002$). The *y*-axis indicates the log10-transformed freezing duration, averaged across six consecutive 5-min bins. Asterisk indicates significant pairwise group differences. Error bars depict s.e.

RESULTS

Identifying stable and extreme BI groups

Across the two phenotyping sessions (Figure 1a), the screening sample of 109 individuals spent more than an order of magnitude more time freezing in response to the human intruder's profile compared with when they were alone in the testing cage (Intruder: *M* (s.d.) = 161.6 s (112.6); Alone: *M* (s.d.) = 14.1 s (24.5)), $F(1,108) = 484.09$, $P < 0.001$). For detailed results, see Supplementary Methods. Individual differences in intruder-elicited freezing were stable over the 1 week interval, $r = 0.74$, $P < 0.001$ (Figure 1b). Using these data, we formed sex- and age-matched groups with stable and extreme levels of the BI phenotype (high BI, low BI; see Table 1 and Supplementary Table S1).

When compared with the low-BI group, the high-BI group showed an 18-fold increase in freezing when the human intruder was present. Additional analyses revealed a 13-fold increase when the high-BI individuals were alone in the testing cage at the beginning of the session (($F(1,21) = 8.56$, $P = 0.008$; see Figure 1a and Supplementary Table S1). In other words, although BI is more strongly expressed in response to the intruder's profile (group × context interaction: $F(1,21) = 13.73$, $P = 0.001$; note: this *P*-value should be interpreted with caution, as this test is not independent of the group-selection procedures), it also manifests in response to the diffusely threatening testing cage.

The BI phenotype shows continuity across time and contexts

To gauge the long-term stability and generality of the BI phenotype, we performed two additional analyses. First, we tested whether the high-BI group continued to show elevated freezing during the first 30 min of the imaging sessions, before FDG administration (Figure 1d). Analyses revealed that subjects froze more in response to the intruder's profile ($F(1,21) = 9.41$, $P = 0.006$) and that the high-BI group froze substantially more than the low-BI group, ($F(1,21) = 10.12$, $P = 0.004$; Supplementary Table S2). In fact, the high-BI group froze >8 times longer than the low-BI group when the intruder was present ($F(1,21) = 10.61$, $P = 0.004$) and nearly five times longer when they were alone in the testing cage ($F(1,21) = 4.99$, $P = 0.04$), despite extensive acclimation to both the cage and testing procedures (Supplementary Methods). Across groups, individual differences in the BI phenotype (that is, intruder-elicited freezing) exhibited substantial test-retest reliability (intraclass correlation = 0.85) over the ~1.5 years separating the phenotyping from the brain imaging sessions (Figure 1).

As a second test of phenotypic continuity, we assessed snake anxiety ~2 years after the initial phenotyping sessions (Figure 1c). Analyses revealed a significant effect of stimulus on anxiety ($F(3,63) = 30.11$, $P < 0.001$). In particular, the frequency of non-responses followed the expected linear pattern: live snake > artificial snake > tape > nothing ($F(1,21) = 62.56$, $P < 0.001$) and all of the pairwise differences between stimuli were in the expected direction and significant ($Ps < 0.03$). Importantly, the group × stimulus interaction was also significant ($F(1,21) = 2.83$, $P < 0.05$). The high-BI group was twice as likely to refrain from reaching for a highly preferred food reward in the presence of the live snake compared with the low-BI group ($F(1,21) = 5.76$, $P = 0.03$). Other differences were not significant ($Ps > 0.20$). Analyses of observer ratings of freezing behavior during the snake anxiety assessment revealed a similar pattern (Supplementary Methods and Supplementary Table S2). Across groups, reticence in the presence of the live snake was prospectively predicted by individual differences in freezing to the intruder's profile during the phenotyping sessions >2 years earlier ($\rho_{Spearman} = 0.44$, $P = 0.04$, $n = 23$). Collectively, these results indicate that the monkey BI phenotype represents an enduring predisposition to respond to a range of potentially threatening cues and contexts with heightened signs of anxiety.

The high-BI group shows persistently elevated freezing following the intruder encounter

Next, we tested whether the high-BI group exhibits persistently elevated freezing following the encounter with the human intruder. Analyses revealed that, on average, subjects froze longer following the intruder encounter ($F(1,21) = 8.20$, $P = 0.009$; Figure 2b and Supplementary Table S2). Consistent with expectation, the group × condition interaction was significant ($F(1,21) = 4.62$, $P = 0.04$). Pairwise contrasts revealed that the high-BI group froze significantly longer during the Alone-following-Intruder condition compared

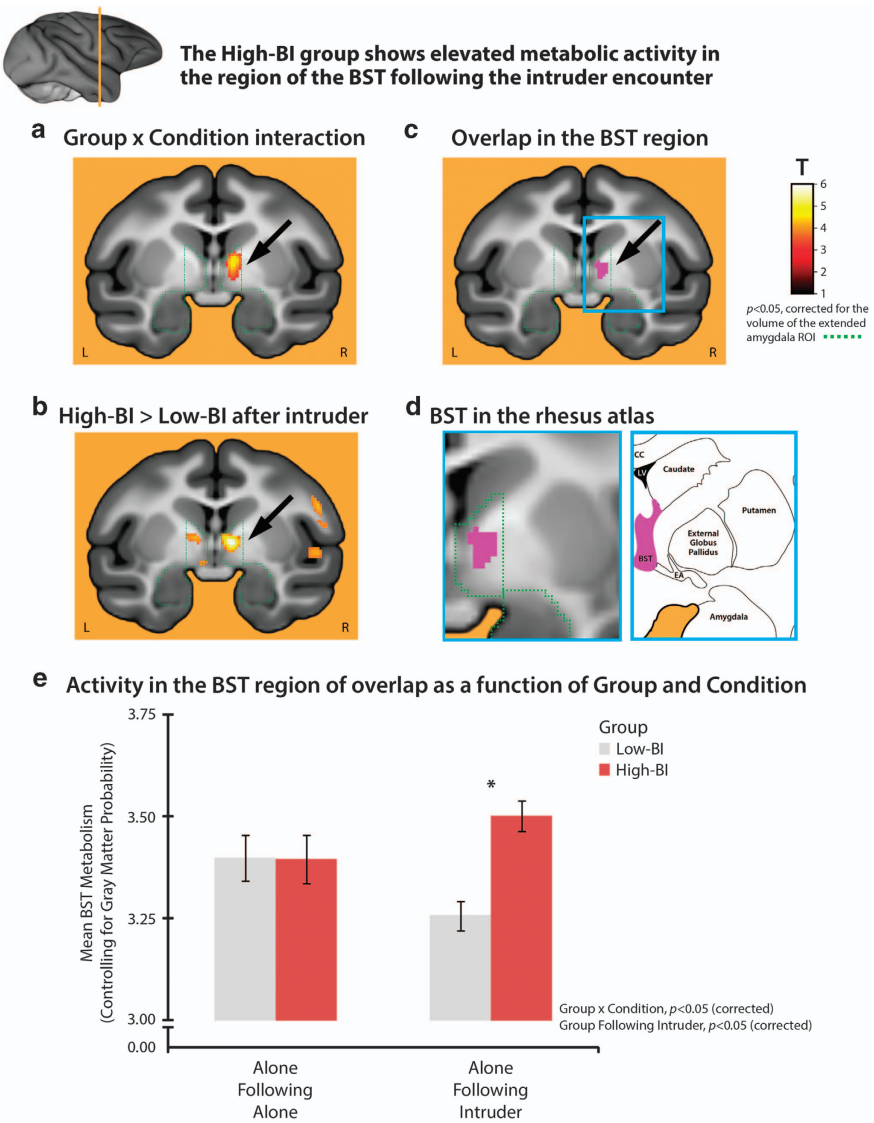

Figure 3. The high-BI (behavioral inhibition) group shows elevated metabolic activity in the region of the bed nucleus of the stria terminalis (BST) following the intruder encounter. The *a priori* extended amygdala region of interest (ROI) is indicated by the dashed green line. The imaging paradigm is depicted in Figure 1d. (**a**) Regions showing a significant group × condition interaction. The cluster in the region of the BST is indicated by the black arrow ($P < 0.05$, small-volume corrected). Data extracted from this cluster is depicted in Supplementary Figure S1. (**b**) Regions where the stable high-BI group showed significantly more activity than the low-BI group during the 30-min 'recovery' period following the intruder encounter. Clusters visually depicted outside the ROI (green) were not significant using a whole-brain threshold. (**c**) Region of overlap in the BST region. A minimum conjunction[44] (logical AND) of the whole-brain contrasts shown in **a** and **b** revealed a cluster in the vicinity of the BST (purple). No other clusters were identified. (**d**) BST in the corresponding region of the rhesus brain atlas. The left image shows a magnified view of the region marked by the cyan rectangle in **c**. The arrow is omitted for clarity. The right image depicts corresponding region of the rhesus atlas. Additional views of the BST clusters can be found in Supplementary Figure S2. (**e**) Activity in the BST region of overlap as a function of group and condition. Figure shows mean activity from the purple cluster depicted in **c** controlling for nuisance variance in mean-centered gray matter probability. Asterisk indicates the significant pairwise group differences. Error bars depict s.e. Portions of this figure were adapted with permission from plate 54 in the atlas of Paxinos *et al*.[73] CC, corpus callosum; EA, extended amygdala; LV, lateral ventricle.

with the Alone-Following-Alone condition ($F(1,21) = 12.04$, $P = 0.002$), whereas the low-BI group did not show significant differences in freezing ($P = 0.61$). This effect was specific to the 'recovery' period following the termination of threat: the high-BI group froze an order of magnitude longer than the low-BI group during the Alone-following-Intruder condition ($F(1,21) = 6.61$, $P = 0.02$), whereas the groups did not significantly differ during the Alone-following-Alone condition ($P = 0.35$). The main effect of group was not significant ($P = 0.08$). These results demonstrate that individuals with stable and extreme BI show sustained levels of heightened anxiety during the half-hour following the intruder encounter.

The high-BI group shows elevated activity in the BST region following the intruder encounter

To identify the neural systems underlying group differences in freezing following the intruder encounter, we used a whole-brain voxelwise general linear models to identify regions where the critical group × condition interaction was significant in the period

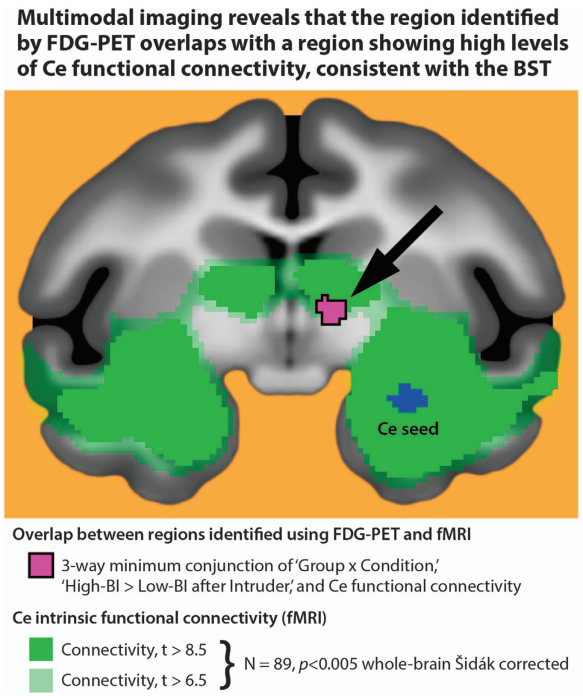

Figure 4. Multimodal imaging reveals that the hypermetabolic region identified by ^{18}fluorodeoxyglucose positron emission tomography (FDG-PET) overlaps a region expressing high levels of Ce functional connectivity, consistent with the bed nucleus of the stria terminalis (BST). Shown in purple is the overlap (that is, minimum conjunction[44]) between voxels identified using FDG-PET (purple cluster in Figure 3c) and those showing significant functional connectivity with the Ce (green) in an independent sample of 89 monkeys (detailed in Birn *et al*.[45]). The substantial overlap enhances our confidence that the hypermetabolic region identified using PET encompasses portions of the BST. The Ce seed region used in the functional connectivity analyses is depicted in blue. BI, behavioral inhibition; fMRI, functional magnetic resonance imaging.

following FDG administration (Figure 1d). Given our *a priori* focus on the extended amygdala, the interaction was thresholded at $P < 0.05$ (corrected for a 4188-voxel region of interest encompassing the amygdala and BST; depicted in green in Figure 3). This analysis revealed a cluster in the region of the BST (Figure 3a; Supplementary Table S3; Supplementary Figure S2). We used a second whole-brain analysis to identify regions where the high-BI group showed significantly more activity than the low-BI group during the Alone-following-Intruder condition ($P < 0.05$, corrected). This revealed an overlapping cluster within the *a priori* region of interest (Figure 3b; Supplementary Table S4). Although several clusters were significant in one or the other of these two statistical maps, the region of overlap in the region of the BST was the only cluster in the entire brain to satisfy both of these critical tests (Figures 3c–e; Supplementary Figure S3). This effect was specific to the period following threat; like freezing behavior, the high- and low-BI groups did not show significant differences in activity in the BST or other regions of the extended amygdala during the control condition (Alone-following-Alone; cf. Figure 3e).

Compared with other brain regions implicated in BI and anxiety, the BST is small and lacks distinct macroscopic boundaries,[33] making it challenging to definitively localize using conventional brain imaging techniques. To better understand the region showing elevated activity in the high-BI group (purple cluster in Figure 3c), we capitalized on work demonstrating that the BST and Ce show robust anatomical[33] and functional connectivity.[45] Here we used previously published[45] fMRI data obtained from an independent sample of 89 young monkeys to demonstrate that the hypermetabolic cluster identified using FDG-PET overlaps with a region expressing high levels of 'resting-state' functional connectivity with the Ce (Figure 4; significant connectivity depicted in green; overlap depicted in purple), enhancing our confidence that it includes the BST.

To clarify the consequences of elevated BST metabolism, we extracted activity from the region of overlap identified using FDG-PET (Figure 3c) for each subject and assessed brain-behavior relations after controlling for nuisance variance in mean-centered gray matter probability. Consistent with the group mean differences described above, individual differences in BST activity following the intruder encounter (a) were prospectively predicted by intruder-elicited freezing during the initial phenotyping sessions (partial $\rho = 0.58$, $P = 0.005$), (b) predicted concurrent freezing (partial $\rho = 0.46$, $P = 0.03$) and (c) discriminated high-BI individuals with good sensitivity (90.9%) and specificity (83.3%), $\chi^2(1) = 15.51$, $P < 0.001$. These relations were specific to the period following the encounter with potential threat; significant associations were not obtained using BST activity associated with the Alone-following-Alone control condition ($Ps > 0.20$). Collectively, these findings suggest that elevated activity in the BST plays a key role in promoting extreme early-life anxiety.

DISCUSSION

The present study, which combines longitudinal phenotyping with high-resolution FDG-PET imaging in young nonhuman primates, provides unique insights into the neural bases of extreme early-life anxiety. Consistent with research in children and adolescents, this work demonstrates that BI represents a trait-like tendency to respond to a range of potentially threatening cues and contexts with increased signs of anxiety. Drawing from a pool of 109 young monkeys, we formed age- and sex-matched groups characterized by stable and extreme freezing in response to an unfamiliar human intruder (Figures 1a and b). Compared with the low-BI group, the high-BI group showed nearly 20 times more freezing to the intruder during the two screening sessions and an order of magnitude more freezing when they re-encountered the intruder ~ 1.5 years later. The high-BI group also showed increased reticence when exposed to a snake ~ 2 years after the initial phenotyping sessions (Figure 1c and Supplementary Methods). In short, the BI phenotype shows continuity across time and across different types of ethologically relevant threats in young monkeys. Importantly, the high-BI group also showed increased freezing when alone in the testing cage during the initial phenotyping sessions and continued to show exaggerated wariness and inhibition in the testing cage during the first 30 min of the brain imaging sessions (that is, before FDG administration), despite repeated exposure to this context during the intervening year-and-a-half. These observations suggest that extreme BI manifests in amplified caution and anxiety in situations where threat is diffuse, weak or uncertain. Consistent with this perspective, the high-BI group showed persistently elevated freezing during the 30-min recovery period following the intruder encounter (Figure 2b)—more than an order of magnitude greater than the low-BI group—and this was associated with increased metabolic activity in the BST region (Figures 3 and 4). Hyper-metabolism was associated with exaggerated freezing and discriminated high- and low-BI individuals with good sensitivity and specificity. Collectively, these observations provide compelling evidence that sustained levels of heightened anxiety in the absence of immediate threat reflect elevated activity in the BST region.

In children, anxious temperament and the narrower BI phenotype are heritable early-life risk factors for the development of anxiety, depression and co-morbid substance abuse[1,2,5] and our results provide a neurobiologically grounded framework for understanding the mechanisms underlying this liability. In particular, our results provide evidence that individuals with

consistently high levels of the BI phenotype early in development show persistent wariness in the period following exposure to potential threat and that this is associated with increased engagement of the BST. These observations complement evidence that threat-elicited activity in the BST is heritable and genetically correlated with individual differences in anxious temperament in young monkeys.[29] The relevance of the BST to sustained anxiety is consistent with anatomical tracing studies in rodents and monkeys showing that this region sends dense projections to brainstem and subcortical effector sites.[33,46] Our imaging results are also consistent with mechanistic studies in rodents showing that the BST exhibits persistent excitability following direct stimulation, supports passive avoidance during sustained exposure (5–20 min) to diffusely threatening contexts (for example, elevated-plus maze), and contributes to the overgeneralization of anxiety to safety cues (CS-).[11,25,26,47,48]

Our observations provide an important extension of recent imaging work documenting that: (a) individuals with extreme anxiety show elevated activation in the vicinity of the BST during exposure to uncertain threat and punishment[49–52] and (b) individual differences in BST function predict anxious mood, freezing, skin conductance and cortisol elicited by uncertain or diffuse threat.[6,28,29,38,53–56] Extending earlier work in rodents, monkeys and humans, our results reflect the comparison of two physically identical conditions (that is, Alone-following-Intruder and Alone-following-Alone; Figure 1d), neural activity integrated over an extended 30 min 'recovery' period following the offset of threat, concurrent measures of naturalistic defensive responses in individuals selected on the basis of stable and extreme phenotypic risk, and a multimodal imaging approach to identifying the BST region. These features enhance our confidence in the translational significance of these results.

Although the BST has not been previously linked to childhood BI, our findings dovetail with emerging evidence that, like anxious adults,[9,11–13] children and adolescents with a history of extreme BI and elevated anxiety are prone to contextually inappropriate defensive behaviors.[14–18,57] Moreover, contextually inappropriate responses in the laboratory prospectively predict heightened real-world anxiety in children and avoidance of threat-related contexts in adults.[19,20] Among adults, heightened apprehension and defensive responses in safe contexts are generally more discriminative of pathological anxiety than that elicited by overt threat.[11,12] This maladaptive phenotype appears to be amplified by early adversity[58] and prospectively predicts the onset of anxiety disorders in adolescence[59] as well as the intensification of anxious symptoms in young adults.[60] Collectively, these findings underscore the potential etiological significance of heightened BST activity.

The BST is increasingly conceptualized as a key promoter of 'sustained' defensive responses to uncertain, psychologically diffuse or temporally remote threat and our results are broadly consistent with this perspective. Nonetheless, it is likely that the BST makes a broader contribution to phenotypic risk and anxiety, one that encompasses exaggerated defensive responses during both sustained and transient exposure to uncertain threat.[24,33,61] Mechanistic work in rodents suggests that BST engagement can begin quite early, between 4 and 60 s following the onset of cues associated with uncertain danger,[11] and contributes to the overgeneralization of conditioned fear to 30 s auditory cues.[25] In human fMRI studies, BST activation has also been observed in response to acute aversive challenges (for example, 4-s tarantula video clip; see refs. 62–65). In fact, a recent meta-analysis demonstrated that imaging studies of fear and anxiety consistently reveal activation in the region of the central extended amygdala, including the BST as well as the Ce, across a broad spectrum of populations, paradigms and time scales.[33] An important avenue for future research will be to clarify the boundary conditions and mechanistic importance of BST engagement.[24] Likewise, while our results highlight the importance of the BST, it will be important to understand how functional interactions between the BST and other regions sensitive to potential threat (for example, Ce, periaqueductal gray, orbitofrontal cortex, insula and anterior cingulate) control the expression of persistent anxiety, support variation in early phenotypic risk and ultimately contribute to the development and maintenance of psychopathology in humans.[24,29,54,66–68] Given the higher prevalence of anxiety disorders and depression among women,[69,70] understanding potential sex differences in the function of these circuits and their relevance to risk represents another key challenge.

As we and other commentators have recently noted, understanding the BST is challenging.[24,33,71] From a technical standpoint, the BST is small; it is functionally and anatomically heterogeneous; and it lacks clear boundaries *in vivo*, even when using ultra-high field-strength MRI techniques.[33,72–75] Furthermore, most imaging software for automated cluster labeling does not include the BST, although standardized segmentation protocols[75] and masks have recently become available (https://afni.nimh.nih.gov/afni/community/board/read.php?1,149436,149436). The upshot is that researchers may not recognize that a cluster encompasses the BST or may be hesitant to label it as such. Regardless of the label, there is value to discussing the potential role of the BST and other neighboring regions of the basal forebrain (for example, accumbens), even in cases where a cluster cannot be unambiguously ascribed to the BST. Using multi-band imaging sequences and high-precision spatial normalization techniques would provide enhanced spatial resolution.[29,76] Multimodal 'double-labeling' strategies, as in the present study (that is, FDG-PET paired with resting-state fMRI) and other recent work by our group[29] (that is, FDG-PET paired with *in vivo* dopamine receptor imaging) provide other tools for ascertaining whether a cluster is likely to include the BST.

Our results also have implications for theories of temperament and personality.[9,77] There is ample evidence that individuals who are most at risk for developing a mood or anxiety disorder are prone to persistently elevated distress in contexts where threat is distant or absent.[78,79] In fact, longitudinal experience-sampling studies suggest that the vast majority of negative affect experienced by adults with an anxious disposition cannot be attributed to clear-cut stressors in the immediate environment.[80] Although this has been described as a tonic or endogenous effect of temperament,[78] our results suggest that it may reflect increased reactivity to stressors that are weak, diffuse (cf. the test cage) or temporally remote (cf. the Alone-following-Intruder condition). Our results and others[33] motivate the hypothesis that this pervasive anxiety partially reflects alterations in BST function.

CONCLUSIONS

The present study demonstrates that individuals with stable and extreme BI respond to a range of potentially threatening cues and contexts with exaggerated defensive responses. Young monkeys with elevated levels of BI consistently over-reacted to both overt and more diffuse kinds of threat during more than two years of longitudinal study. Concurrent measures of FDG metabolism provide unique evidence that heightened defensive responses following an encounter with potential threat reflects increased engagement of the BST, a key component of the central extended amygdala. The present study has several features that enhance our confidence in the translational significance of these results, including the use of a well-validated primate model of early-life anxiety, physically identical 'recovery' conditions,[81,82] concurrent measures of evolutionarily conserved emotional behaviors, and a multimodal approach to identifying the BST. Translational brain imaging strategies, like that featured in the present study, provide a powerful tool for bridging the gap separating the mechanistic insights afforded by nonhuman animal models from

the complexity of human emotions, temperament, and psychopathology and accelerating therapeutic development. Developing more effective interventions is particularly important for minimizing the cumulative damage associated with extreme BI and anxiety early in development.

CONFLICT OF INTEREST

The authors declare no conflict of interest.

ACKNOWLEDGMENTS

Authors acknowledge assistance and critical feedback from A Alexander, A Converse, L Friedman, D Grupe, R Hoks, T Johnson, S Mansavage, K Meyer, L Pessoa, D Pine, P Rudebeck, W Shelledy, M Stockbridge, T Johnstone, E Zao and the staffs of the Harlow Center for Biological Psychology, HealthEmotions Research Institute (HERI), and Wisconsin National Primate Center. We are particularly grateful for the contributions of Helen Van Valkenberg to this work. This work was supported by the National Institutes of Health (DA040717, HD003352, HD008352, MH018931, MH046729, MH069315, MH081884, MH084051, MH091550, MH107444, OD011106 and RR000167), HERI, Meriter Hospital and University of Maryland.

AUTHOR CONTRIBUTIONS

NHK and SES designed the study. RJD provided theoretical guidance. SES collected data. ASF processed data. AJS, ASF, TRO and NHK analyzed data. ASF and TRO developed analytical tools. AJS, ASF, NHK, JAO and RJD contributed to data interpretation. AJS, ASF and NHK wrote the paper. AJS and ASF created figures and tables. NHK supervised the study. All authors reviewed and revised the paper

REFERENCES

1 Clauss JA, Blackford JU. Behavioral inhibition and risk for developing social anxiety disorder: a meta-analytic study. *J Am Acad Child Adolesc Psychiatry* 2012; **51**: 1066–1075.
2 Pine DS, Fox NA. Childhood antecedents and risk for adult mental disorders. *Annu Rev Psychol* 2015; **66**: 459–485.
3 Insel TR. Next-generation treatments for mental disorders. *Sci Transl Med* 2012; **4**: 155ps119.
4 Kagan J, Reznick JS, Snidman N. Biological bases of childhood shyness. *Science* 1988; **240**: 167–171.
5 Fox AS, Kalin NH. A translational neuroscience approach to understanding the development of social anxiety disorder and its pathophysiology. *Am J Psychiatry* 2014; **171**: 1162–1173.
6 Fox AS, Shelton SE, Oakes TR, Davidson RJ, Kalin NH. Trait-like brain activity during adolescence predicts anxious temperament in primates. *PLoS ONE* 2008; **3**: e2570.
7 Oler JA, Fox AS, Shackman AJ, Kalin NH. The central nucleus of the amygdala is a critical substrate for individual differences in anxiety. In: Amaral DG, Adolphs R (eds). *Living Without an Amygdala*. Guilford: NY, 2016.
8 Buss KA, Kiel EJ. Temperamental risk factors for pediatric anxiety disorders. In: Vasa RA, Roy AK (eds). *Pediatric Anxiety Disorders: A Clinical Guide*. Springer: NY, 2013, pp 47–68.
9 Shackman AJ, Tromp DPM, Stockbridge MD, Kaplan CM, Tillman RM, Fox AS. Dispositional negativity: an integrative psychological and neurobiological perspective. *Psychol Bull* (in press).
10 Davidson RJ, Jackson DC, Kalin NH. Emotion, plasticity, context, and regulation: Perspectives from affective neuroscience. *Psychol Bull* 2000; **126**: 890–909.
11 Davis M, Walker DL, Miles L, Grillon C. Phasic vs sustained fear in rats and humans: role of the extended amygdala in fear vs anxiety. *Neuropsychopharmacology* 2010; **35**: 105–135.
12 Duits P, Cath DC, Lissek S, Hox JJ, Hamm AO, Engelhard IM *et al.* Updated meta-analysis of classical fear conditioning in the anxiety disorders. *Depress Anxiety* 2015; 239–253.
13 Grupe DW, Nitschke JB. Uncertainty and anticipation in anxiety: an integrated neurobiological and psychological perspective. *Nat Rev Neurosci* 2013; **14**: 488–501.
14 Barker TV, Reeb-Sutherland BC, Fox NA. Individual differences in fear potentiated startle in behaviorally inhibited children. *Dev Psychobiol* 2014; **56**: 133–141.
15 Reeb-Sutherland BC, Helfinstein SM, Degnan KA, Perez-Edgar K, Henderson HA, Lissek S *et al.* Startle response in behaviorally inhibited adolescents with a lifetime occurrence of anxiety disorders. *J Am Acad Child Adolesc Psychiatry* 2009; **48**: 610–617.
16 Waters AM, Nazarian M, Mineka S, Zinbarg RE, Griffith JW, Naliboff B *et al.* Context and explicit threat cue modulation of the startle reflex: preliminary evidence of distinctions between adolescents with principal fear disorders versus distress disorders. *Psychiatry Res* 2014; **217**: 93–99.
17 Jovanovic T, Nylocks KM, Gamwell KL, Smith A, Davis TA, Norrholm SD *et al.* Development of fear acquisition and extinction in children: effects of age and anxiety. *Neurobiol Learn Mem* 2014; **113**: 135–142.
18 Reznick JS, Kagan J, Snidman N, Gersten M, Baak K, Rosenberg A. Inhibited and uninhibited children: A follow-up study. *Child Dev* 1986; **57**: 660–680.
19 Buss KA, Davis EL, Kiel EJ, Brooker RJ, Beekman C, Early MC. Dysregulated fear predicts social wariness and social anxiety symptoms during kindergarten. *J Clin Child Adolesc Psychol* 2013; **42**: 603–616.
20 Grillon C. Associative learning deficits increase symptoms of anxiety in humans. *Biol Psychiatry* 2002; **51**: 851–858.
21 Houben M, Van Den Noortgate W, Kuppens P. The relation between short-term emotion dynamics and psychological well-being: a meta-analysis. *Psychol Bull* 2015; **141**: 901–930.
22 Newman MG, Fisher AJ. Mediated moderation in combined cognitive behavioral therapy versus component treatments for generalized anxiety disorder. *J Consult Clin Psychol* 2013; **81**: 405–414.
23 van de Leemput IA, Wichers M, Cramer AO, Borsboom D, Tuerlinckx F, Kuppens P *et al.* Critical slowing down as early warning for the onset and termination of depression. *Proc Natl Acad Sci USA* 2014; **111**: 87–92.
24 Shackman AJ, Fox AS. Contributions of the central extended amygdala to fear and anxiety. *J Neurosci*; **36**: 8050–8063.
25 Duvarci S, Bauer EP, Pare D. The bed nucleus of the stria terminalis mediates inter-individual variations in anxiety and fear. *J Neurosci* 2009; **29**: 10357–10361.
26 Kim SY, Adhikari A, Lee SY, Marshel JH, Kim CK, Mallory CS *et al.* Diverging neural pathways assemble a behavioural state from separable features in anxiety. *Nature* 2013; **496**: 219–223.
27 Botta P, Demmou L, Kasugai Y, Markovic M, Xu C, Fadok JP *et al.* Regulating anxiety with extrasynaptic inhibition. *Nat Neurosci* 2015; **18**: 1493–1500.
28 Shackman AJ, Fox AS, Oler JA, Shelton SE, Davidson RJ, Kalin NH. Neural mechanisms underlying heterogeneity in the presentation of anxious temperament. *Proc Natl Acad Sci USA* 2013; **110**: 6145–6150.
29 Fox AS, Oler JA, Shackman AJ, Shelton SE, Raveendran M, McKay DR *et al.* Intergenerational neural mediators of early-life anxious temperament. *Proc Natl Acad Sci USA* 2015; **112**: 9118–9122.
30 Fox NA, Henderson HA, Marshall PJ, Nichols KE, Ghera MM. Behavioral inhibition: linking biology and behavior within a developmental framework. *Annu Rev Psychol* 2005; **56**: 235–262.
31 Gibbs RA, Rogers J, Katze MG, Bumgarner R, Weinstock GM, Mardis ER *et al.* Evolutionary and biomedical insights from the rhesus macaque genome. *Science* 2007; **316**: 222–234.
32 Preuss TM. Primate brain evolution in phylogenetic context. In: Kaas JH, Preuss TM (eds). *Evolution of Nervous Sytems*, vol. 4. Elsevier: NY, 2007, pp 3–34.
33 Fox AS, Oler JA, Tromp DP, Fudge JL, Kalin NH. Extending the amygdala in theories of threat processing. *Trends Neurosci* 2015; **38**: 319–329.
34 deCampo DM, Fudge JL. Amygdala projections to the lateral bed nucleus of the stria terminalis in the macaque: comparison with ventral striatal afferents. *J Comp Neurol* 2013; **521**: 3191–3216.
35 Kalin NH, Shelton SE. Defensive behaviors in infant rhesus monkeys: environmental cues and neurochemical regulation. *Science* 1989; **243**: 1718–1721.
36 Rilling JK, Winslow JT, O'Brien D, Gutman DA, Hoffman JM, Kilts CD. Neural correlates of maternal separation in rhesus monkeys. *Biol Psychiatry* 2001; **49**: 146–157.
37 Kalin NH, Shelton SE, Fox AS, Rogers J, Oakes TR, Davidson RJ. The serotonin transporter genotype is associated with intermediate brain phenotypes that depend on the context of eliciting stressor. *Mol Psychiatry* 2008; **13**: 1021–1027.
38 Jahn AL, Fox AS, Abercrombie HC, Shelton SE, Oakes TR, Davidson RJ *et al.* Subgenual prefrontal cortex activity predicts individual differences in hypothalamic-pituitary-adrenal activity across different contexts. *Biol Psychiatry* 2010; **67**: 175–181.
39 Oler JA, Fox AS, Shelton SE, Christian BT, Murali D, Oakes TR *et al.* Serotonin transporter availability in the amygdala and bed nucleus of the stria terminalis predicts anxious temperament and brain glucose metabolic activity. *J Neurosci* 2009; **29**: 9961–9966.
40 Preacher KJ, Rucker DD, MacCallum RC, Nicewander WA. Use of the extreme groups approach: a critical reexamination and new recommendations. *Psychol Methods* 2005; **10**: 178–192.
41 Kalin NH, Shelton SE, Davidson RJ. Role of the primate orbitofrontal cortex in mediating anxious temperament. *Biol Psychiatry* 2007; **62**: 1134–1139.
42 Kalin NH, Shelton SE, Davidson RJ. The role of the central nucleus of the amygdala in mediating fear and anxiety in the primate. *J Neurosci* 2004; **24**: 5506–5515.

43 Chronis-Tuscano A, Degnan KA, Pine DS, Perez-Edgar K, Henderson HA, Diaz Y *et al.* Stable early maternal report of behavioral inhibition predicts lifetime social anxiety disorder in adolescence. *J Am Acad Child Adolesc Psychiatry* 2009; **48**: 928–935.
44 Nichols T, Brett M, Andersson J, Wager T, Poline JB. Valid conjunction inference with the minimum statistic. *Neuroimage* 2005; **25**: 653–660.
45 Birn RM, Shackman AJ, Oler JA, Williams LE, McFarlin DR, Rogers GM *et al.* Evolutionarily-conserved dysfunction of prefrontal-amygdalar connectivity in early-life anxiety. *Mol Psychiatry* 2014; **19**: 915–922.
46 Davis M, Whalen PJ. The amygdala: vigilance and emotion. *Mol Psychiatry* 2001; **6**: 13–34.
47 Walker DL, Davis M. Role of the extended amygdala in short-duration versus sustained fear: a tribute to Dr. Lennart Heimer. *Brain Struct Funct* 2008; **213**: 29–42.
48 Nagy FZ, Pare D. Timing of impulses from the central amygdala and bed nucleus of the stria terminalis to the brain stem. *J Neurophysiol* 2008; **100**: 3429–3436.
49 Somerville LH, Whalen PJ, Kelley WM. Human bed nucleus of the stria terminalis indexes hypervigilant threat monitoring. *Biol Psychiatry* 2010; **68**: 416–424.
50 Straube T, Mentzel HJ, Miltner WHR. Waiting for spiders: Brain activation during anticipatory anxiety in spider phobics. *Neuroimage* 2007; **37**: 1427–1436.
51 Yassa MA, Hazlett RL, Stark CE, Hoehn-Saric R. Functional MRI of the amygdala and bed nucleus of the stria terminalis during conditions of uncertainty in generalized anxiety disorder. *J Psychiatr Res* 2012; **46**: 1045–1052.
52 Munsterkotter AL, Notzon S, Redlich R, Grotegerd D, Dohm K, Arolt V *et al.* Spider or no spider? Neural correlates of sustained and phasic fear in spider phobia. *Depress Anxiety* 2015; **32**: 656–663 (in press).
53 Kalin NH, Shelton SE, Fox AS, Oakes TR, Davidson RJ. Brain regions associated with the expression and contextual regulation of anxiety in primates. *Biol Psychiatry* 2005; **58**: 796–804.
54 Somerville LH, Wagner DD, Wig GS, Moran JM, Whalen PJ, Kelley WM. Interactions between transient and sustained neural signals support the generation and regulation of anxious emotion. *Cereb Cortex* 2013; **23**: 49–60.
55 McMenamin BW, Langeslag SJ, Sirbu M, Padmala S, Pessoa L. Network organization unfolds over time during periods of anxious anticipation. *J Neurosci* 2014; **34**: 11261–11273.
56 Alvarez RP, Kirlic N, Misaki M, Bodurka J, Rhudy JL, Paulus MP *et al.* Increased anterior insula activity in anxious individuals is linked to diminished perceived control. *Transl Psychiatry* 2015; **5**: e591.
57 Buss KA. Which fearful toddlers should we worry about? Context, fear regulation, and anxiety risk. *Dev Psychol* 2011; **47**: 804–819.
58 Wolitzky-Taylor K, Vrshek-Schallhorn S, Waters AM, Mineka S, Zinbarg R, Ornitz E *et al.* Adversity in early and mid-adolescence is associated with elevated startle responses to safety cues in late adolescence. *Clin Psychol Sci* 2014; **2**: 202–213.
59 Craske MG, Wolitzky-Taylor KB, Mineka S, Zinbarg R, Waters AM, Vrshek-Schallhorn S *et al.* Elevated responding to safe conditions as a specific risk factor for anxiety versus depressive disorders: evidence from a longitudinal investigation. *J Abnorm Psychol* 2012; **121**: 315–324.
60 Lenaert B, Boddez Y, Griffith JW, Vervliet B, Schruers K, Hermans D. Aversive learning and generalization predict subclinical levels of anxiety: a six-month longitudinal study. *J Anxiety Disord* 2014; **28**: 747–753.
61 LeDoux JE. *Anxious: Using the Brain to Understand and Treat Fear and Anxiety*. Viking: NY, 2015.
62 Mobbs D, Yu R, Rowe JB, Eich H, FeldmanHall O, Dalgleish T. Neural activity associated with monitoring the oscillating threat value of a tarantula. *Proc Natl Acad Sci USA* 2010; **107**: 20582–20586.
63 Grupe DW, Oathes DJ, Nitschke JB. Dissecting the anticipation of aversion reveals dissociable neural networks. *Cereb Cortex* 2013; **23**: 1874–1883.
64 Choi JM, Padmala S, Pessoa L. Impact of state anxiety on the interaction between threat monitoring and cognition. *Neuroimage* 2012; **59**: 1912–1923.
65 Klumpers F, Kroes MC, Heitland I, Everaerd D, Akkermans SE, Oosting RS *et al.* Dorsomedial prefrontal cortex mediates the impact of serotonin transporter linked polymorphic region genotype on anticipatory threat reactions. *Biol Psychiatry* 2015; **78**: 582–589.
66 Fox AS, Shelton SE, Oakes TR, Converse AK, Davidson RJ, Kalin NH. Orbitofrontal cortex lesions alter anxiety-related activity in the primate bed nucleus of stria terminalis. *J Neurosci* 2010; **30**: 7023–7027.
67 Shackman AJ, Salomons TV, Slagter HA, Fox AS, Winter JJ, Davidson RJ. The integration of negative affect, pain and cognitive control in the cingulate cortex. *Nat Rev Neurosci* 2011; **12**: 154–167.
68 Mobbs D, Hagan CC, Dalgleish T, Silston B, Prevost C. The ecology of human fear: survival optimization and the nervous system. *Front Neurosci* 2015; **9**: 55.
69 McLean CP, Asnaani A, Litz BT, Hofmann SG. Gender differences in anxiety disorders: prevalence, course of illness, comorbidity and burden of illness. *J Psychiatr Res* 2011; **45**: 1027–1035.
70 Gater R, Tansella M, Korten A, Tiemens BG, Mavreas VG, Olatawura MO. Sex differences in the prevalence and detection of depressive and anxiety disorders in general health care settings: report from the World Health Organization Collaborative Study on Psychological Problems in General Health Care. *Arch Gen Psychiatry* 1998; **55**: 405–413.
71 Avery SN, Clauss JA, Blackford JU. The human BNST: Functional role in anxiety and addiction. *Neuropsychopharmacology* 2016; **41**: 126–141.
72 Mai JK, Paxinos G, Voss T. *Atlas of the Human Brain*, 3rd edn. Academic Press: San Diego, CA, 2007.
73 Paxinos G, Huang X, Petrides M, Toga A. *The Rhesus Monkey Brain in Stereotaxic Coordinates* 2nd edn. Academic Press: San Diego, 2009.
74 Avery SN, Clauss JA, Winder DG, Woodward N, Heckers S, Blackford JU. BNST neurocircuitry in humans. *Neuroimage* 2014; **91**: 311–323.
75 Torrisi S, O'Connell K, Davis A, Reynolds R, Balderston N, Fudge JL *et al.* Resting state connectivity of the bed nucleus of the stria terminalis at ultra-high field. *Hum Brain Mapp* 2015; **36**: 4076–4088.
76 Klein A, Andersson J, Ardekani BA, Ashburner J, Avants B, Chiang MC *et al.* Evaluation of 14 nonlinear deformation algorithms applied to human brain MRI registration. *Neuroimage* 2009; **46**: 786–802.
77 Caspi A, Roberts BW, Shiner RL. Personality development: stability and change. *Annu Rev Psychol* 2005; **56**: 453–484.
78 Gross JJ, Sutton SK, Ketelaar T. Relations between affect and personality: support for the affect-level and affective reactivity views. *Pers Soc Psychol Bull* 1998; **24**: 279–288.
79 Suls J, Martin R. The daily life of the garden-variety neurotic: reactivity, stressor exposure, mood spillover, and maladaptive coping. *J Pers* 2005; **73**: 1485–1509.
80 Bolger N, Schilling EA. Personality and the problems of everyday life: the role of neuroticism in exposure and reactivity to daily stressors. *J Pers* 1991; **59**: 355–386.
81 Luck SJ. Ten simple rules for designing ERP experiments. In: Handy TC (ed). *Event-Related Potentials: A Methods Handbook*. MIT Press: Cambridge, MA, 2005, pp 17–32.
82 Shackman AJ, Sarinopoulos I, Maxwell JS, Pizzagalli DA, Lavric A, Davidson RJ. Anxiety selectively disrupts visuospatial working memory. *Emotion* 2006; **6**: 40–61.
83 Crapse TB, Sommer MA. Corollary discharge across the animal kingdom. *Nat Rev Neurosci* 2008; **9**: 587–600.
84 Maren S, Phan KL, Liberzon I. The contextual brain: implications for fear conditioning, extinction and psychopathology. *Nat Rev Neurosci* 2013; **14**: 417–428.

Supplementary Information accompanies the paper on the Molecular Psychiatry website (http://www.nature.com/mp)

Supplementary Method and Results to Accompany
AJ Shackman, AS Fox, JA Oler, SE Shelton, TR Oakes, RJ Davidson & NH Kalin

SECTION	**PAGE**
Subjects	2
Study Overview	2
Formation of Groups with Stable and Extreme Levels of the BI Phenotype	3
Snake Anxiety	3
Habituation to the Imaging Procedures	4
FDG-PET Data Acquisition	4
MRI Data Acquisition	4
Brain Imaging Data Processing Pipeline	4
Brain Imaging Hypothesis Testing Strategy	5
Test-Retest Reliability of the BI Phenotype	6
The High-BI Group Shows Elevated Freezing in the Presence and Absence of Threat During the Screening Sessions	6
The High-BI Group Shows Elevated Freezing in Response to the Live Snake and Perceptually-Similar Control Stimuli	7
Exploratory Analyses of Response Time (RT) During the Snake Anxiety Assessment	8
Supplementary Table S1	9
Supplementary Table S2	10
Supplementary Table S3	11
Supplementary Table S4	12
Supplementary Figure 1	13
Supplementary Figure 2	14
Supplementary Figure 2	15
Supplementary References	16

Please Address Correspondence to:
Ned H. Kalin (nkalin@wisc.edu)
HealthEmotions Research Institute and Wisconsin Psychiatric Institute & Clinics
University of Wisconsin—Madison
6001 Research Park Boulevard
Madison, Wisconsin 53719 USA

Subjects

Young rhesus monkeys (*Macaca mulatta*; *n*=109; 63.3% female; *M* (*SD*)=2.19 years (.50); range=1.45-3.42 years) were tested as part of a larger program of research focused on the mechanisms underlying extreme early-life anxiety[1-4]. This sample can be considered peri-adolescent; macaques typically become sexually mature between 3 and 4 years of age[5]. Data were collected between September 2004 and November 2006. Hypothesis testing focused on data obtained from 23 animals selected on the basis of stable and extreme levels of freezing (High-BI: *n*=11; Low-BI: *n*=12; **Table 1**), a core component of what we and others have termed 'behavioral inhibition' or 'anxious temperament'[2, 6]. We focused on freezing behavior because, in contrast to other components of anxious temperament (e.g. cortisol), it affords the temporal resolution needed to dissociate recovery from the acute impact of exposure to the intruder's profile (cf. **Figure 1d**). Procedures were in accord with guidelines established by the local Institutional Animal Care and Use Committee.

Study Overview

Behavioral, brain imaging, and neuroendocrine techniques are detailed in prior publications[1-4, 6-10]. In brief, variation in freezing (≥3-seconds characterized by a tense body posture and the absence of vocalizations or movements other than slow head movements or eye-blinks) elicited by threat was assessed in 109 monkeys on two occasions, one week apart using the No-Eye Contact (NEC) condition of the Human Intruder Paradigm[7, 10, 11] (**Figure 1a**). Similar to procedures used for assessing BI in children[12-14], a human intruder entered the room and stood motionless ~2.5 meters from the testing cage while presenting his profile and avoiding eye-contact. Experimental personnel were blind to group status at the time of data collection. Using these data, we formed age- and sex-matched groups with stable high (*n*=11), middle (*n*=12), or low (*n*=12) levels of BI (**Figure 1b and Table 1**). Following the second phenotyping session, only the two extreme BI groups were further assessed. To assess the long-term stability and generality of BI, snake anxiety was assessed in a follow-up session, approximately 2 years after initial phenotyping (**Figure 1c**).

The central aim of the present study was to understand the substrates of maladaptively persistent, context-inappropriate defensive responses following an encounter with an ethologically-relevant threat. Accordingly, the High- and Low-BI groups (but not the Middle-BI group) completed two brain imaging sessions, termed *Alone-Following-Intruder* and *Alone-Following-Alone* (order counterbalanced; mean [*SD*] inter-session interval: 2.20 (1.10) weeks). At the start of each imaging session, subjects were separated

from their cage-mate and transported to a testing cage. The remainder of the session was organized into two 30-min halves. In the first half, groups were either exposed to the human intruder's profile or were placed alone in the testing cage. To minimize habituation, the intruder presented his profile for 10 min, exited the testing environment, returned after 5 min, presented his profile for 5 min, exited for 5 min, and then presented for a final 5 min. Subjects then received a manual injection of <10 mCi of ^{18}FDG via a 19 gauge intravenous catheter in the saphenous vein. Critically, this procedure allowed us to assess brain metabolic activity during the second half of the session, a 30-min 'recovery' period in which subjects were alone and allowed to freely behave in the testing cage. At the end of the second half hour, subjects were anesthetized and scanned. Higher FDG-PET signals reflect greater regional brain metabolism during the physically-identical 30-min 'recovery' periods (i.e. Alone-Following-Intruder or Alone-Following-Alone). Incorporating the Alone-Following-Alone condition also allowed us to control for time spent in the testing cage (i.e. habituation) and residual distress elicited by FDG administration. To be explicit, brain activity associated with the first half of the session was not measured. Structural MRI data were collected during a separate session.

Formation of Groups with Stable and Extreme Levels of the BI Phenotype

Research in children indicates that those who consistently express high levels of freezing, wariness, and reticence across repeated assessments are at the greatest risk for developing anxiety disorders[15-19]. Accordingly, in the present study, groups with stable and extreme BI were formed by organizing subjects into quartiles based on $\log_{10}$-transformed freezing during the NEC challenge for the first, second, and mean of the two initial phenotyping sessions. Subjects who remained in the same quartile across all three metrics were deemed stable (Stable-High: 10 females and 6 males; Stable-Low: 15 females and 5 males). Age- and sex-matched extreme-BI groups (n=12; 9 female) were formed using the most extreme individuals with stable phenotypes. In contrast to post-hoc dichotomization, the use of extreme groups is scientifically and statistically appropriate[20]. One subject assigned to the High-BI group was removed from the study by veterinary staff because she consistently refused to leave her home cage (for additional details, see Ref. [6]). During the initial phenotyping sessions, freezing was also assessed in the absence of potential threat (i.e. the 'Alone' condition of the Human Intruder Paradigm[7, 10]). The Alone condition was always administered first to circumvent carry-over from the higher-intensity intruder challenge.

Snake Anxiety

To clarify the longer-term stability and generality of the BI phenotype, snake anxiety was assessed using standard techniques[8, 21, 22]. In brief, subjects were habituated to the Wisconsin General Testing Apparatus

(WGTA) and individual differences in food preferences (e.g. raisins) were determined. Subjects were then trained to rapidly retrieve highly-preferred foods (e.g. chocolate chips).. During the anxiety assessment, the two most preferred foods were presented on top of a clear plastic box (side counterbalanced across trials) containing a live snake (*pituophis melanoleucus*), a 120-cm black-rubber artificial snake, a roll of blue masking tape, or nothing (6 60-s trials/condition; order counterbalanced across subjects; 45-s inter-trial interval). The live snake was never presented during the first five trials and none of the conditions was presented for more than three consecutive trials. Non-responses, response times (RT), and freezing behavior (≥3-seconds characterized by a tense body posture and the absence of vocalizations or movements other than slow head movements or eye-blinks) were recorded by an experienced observer. Given the substantial number of non-responses in the live snake condition, the total number of square-root-transformed non-responses was used as the primary dependent measure of snake anxiety. This metric circumvented the need to omit subjects with incomplete RT data, maximizing statistical power.

Habituation to the Imaging Procedures

Subjects in the two extreme groups were acclimated to the experimental procedures prior to the first imaging session. Specifically, they were placed in the testing cage (10 min), moved to the squeeze cage used for FDG injection (8 min), and then returned to the testing cage (10 min) once a day for five consecutive days.

FDG-PET Data Acquisition

At the end of the second half of the brain imaging session, subjects were deeply anesthetized (15mg/kg ketamine i.m.), intubated, and positioned in a stereotactic device within a Siemens/Concorde microPET P4 scanner[23]. Both FDG and attenuation scans were acquired. FDG-PET measures of regional activity reflect the amount of FDG uptake and metabolism between the injection and the scan; regions that are more metabolically active during the behavioral challenge take up more radio-labeled glucose. General anesthesia was maintained using 1-2% isoflurane gas. Images were reconstructed using standard filtered-backprojection techniques with attenuation- and scatter-correction and scaled to a global mean of 5.

MRI Data Acquisition

MRI data were collected under anesthesia using a General Electric (GE) SIGNA 3T MRI scanner (GE Healthcare, Waukesha, WI) equipped with a standard 16-cm quadrature coil. Subjects were anesthetized with ketamine (15 mg/kg delivered intramuscularly), placed in a stereotactic head-frame integrated with

the coil, and positioned in the scanner. Just prior to the start of the first scan, subjects received medetomidine (30 μg/kg delivered intramuscularly). Small doses of ketamine were administered as needed to maintain anesthesia (<15 mg/kg). Anatomical scans were obtained with a 3D T1-weighted, inversion-recovery, gradient-echo prescription (TI/TR/TE/Flip/NEX/FOV/Matrix/Bandwidth/Slices/Gap: 600ms/8.648ms/1.888ms/10°/2/140mm/256 × 224/61.0547kHz/128/-0.5mm; reconstructed on the scanner to 0.2734×0.2734×0.5 mm).

Brain Imaging Data Processing Pipeline

Prior to spatial normalization, brains were manually extracted from T1 images using SPAMALIZE (http://psyphz.psych.wisc.edu/~oakes/spam). To generate the study-specific template, native-space, brain-extracted T1 images were linearly registered (9-*df*) to a pre-existing template[2] in the stereotactic space of Paxinos and colleagues[24] using FLIRT (http://fsl.fmrib.ox.ac.uk/fsl/flirt). Images were visually inspected and averaged to create an age-appropriate template interpolated to 0.625-mm^3 voxels. Native-space, brain-extracted T1 images were registered to the study-specific template (12-*df* linear and 5th-order nonlinear transformations) using AIR (http://bishopw.loni.ucla.edu/air5) and segmented into gray matter (GM), white matter (WM), and cerebrospinal fluid (CSF) using FAST (http://www.fmrib.ox.ac.uk/fsl/fast4).

PET images were registered to the corresponding native-space T1 images using subject-specific PET templates. Specifically, single-subject PET images were linearly registered (6-*df*) to the first PET image acquired for that individual using FLIRT. The registered images were averaged to create subject-specific PET templates. Native-space single-subject PET images were then linearly registered to the corresponding template using AIR and averaged. The registered and averaged single-subject PET image was linearly registered to the corresponding native-space T1 image. The resulting transformation matrices were concatenated with those defining the nonlinear transformation to the template and used to spatially normalize and interpolate the PET images to the 0.625-mm^3 template. Normalized PET images were global-mean scaled within the brain using SPAMALIZE. Scaled PET and GM probability maps were spatially smoothed (4mm FWHM Gaussian). All data were visually inspected to ensure accurate preprocessing.

Brain Imaging Hypothesis Testing Strategy

Behavioral data were analyzed using standard general linear models (GLM) implemented In SPSS (version 23; IBM Inc., Armonk, NY) with Huynh-Feldt correction as required. For the FDG-PET data, we used a series of whole-brain voxelwise general linear models (GLM) to identify regions (i) where the Group (High-BI, Low-BI) × Condition (Alone-Following-Intruder, Alone-Following-Alone) interaction was significant and (ii) where the High-BI group showed significantly more metabolism than the Low-BI group during the critical 30-min 'recovery' period following the threat encounter (Alone-Following-Intruder). Both tests were conducted using MULTISTATIC[25], an extension of FMRISTAT (http://www.math.mcgill.ca/keith/fmristat), and controlled for nuisance variation in mean-centered voxelwise GM probability (GMP), an indirect measure of differences in spatial normalization and gross anatomy[25]. Given our *a priori* focus on the potential contributions of the amygdala and BST, each test was thresholded at $p<.05$, corrected for the extent of a 4,188-voxel region-of-interest (ROI) encompassing both regions bilaterally. This threshold (94 voxels or 22.9 mm^3) was computed based on a voxelwise threshold of $p<.005$ using Monte Carlo techniques implemented in AFNI (http://afni.nimh.nih.gov)[26]. The ROI was manually prescribed based on Ref. [24]. To formally identify regions satisfying both criteria, the two thresholded statistical maps were combined using a two-way minimum conjunction test (i.e. logical AND)[27]. To provide additional information about specificity, clusters outside of the ROI that survived the small-volume threshold are depicted visually and reported in the supplementary tables (i.e. are not masked). Only one of these clusters was significant after correcting for whole-brain analyses (867 voxels or 211.7 mm^3). Follow-up tests of brain-behavior relations were performed using regression and classifier models implemented in SPSS version 23 (IBM Inc., Armonk, NY) and controlling for nuisance variation in GMP. For the discriminant analysis predicting group membership based on brain activity, sensitivity and specificity were computed using leave-one-out cross-validation. Diagnostic tests confirmed that these individual differences data satisfied the relevant GLM assumptions (e.g., the residuals were normally distributed). Some figures were created using MRIcron (http://www.mccauslandcenter.sc.edu/mricro/mricron) or Scatterize (http://webtasks.keck.waisman.wisc.edu/scatterize).

Test-Retest Reliability of the BI Phenotype

Across all subjects, the one-week stability of intruder-elicited freezing across the two initial phenotyping sessions was good, $r=.74$, $p<.001$. Across the two extreme groups ($n=23$), individual differences in intruder-elicited freezing showed good test-retest reliability between the two initial phenotyping sessions and the imaging sessions, $ICC_{3,k}=.85$ (*M* (*SD*) interval=1.62 (.06) years). The bivariate correlation

between differences in freezing averaged across the two phenotyping sessions and the first exposure to intruder threat during the imaging sessions was r=.56, p=.006.

These levels of stability are comparable to those obtained for self-report measures of negative affect and other emotional traits in adult humans over similar spans[28]. The true psychometric reliability of the BI phenotype in monkeys is likely to be somewhat higher because of the lengthy span of time between the first and the third measurements[29] and the fact that data were acquired early in life, a time of substantial neural and psychological change[30, 31].

The High-BI Group Shows Elevated Freezing in the Presence and Absence of Threat During the Screening Sessions

Based on the data obtained during the two screening sessions, we formed age- and sex-matched groups with stable and extreme levels of BI (High-BI, Low-BI; see **Table 1** in the main report; details are group formation are described above). For comparison purposes, we also created a group with typical levels of BI (Middle-BI). For completeness, here we report the results of analyses comparing these three groups. However, is important to emphasize that these are 'circular' or 'non-independent' analyses[32, 33] insofar as the groups were formed using the same data employed in these inferential tests. As a consequence, the results and accompanying p-values are biased.

Analyses revealed that exposure to the human intruder's profile increased freezing, $F(1,32)=168.89$, $p<.001$. All three groups showed an approximately eleven-fold increase in freezing when threat was present ($ps<.001$; **see Table S1**). This increase was more pronounced during the first ($F(1,32)=159.65$, $p<.001$) compared to the second phenotyping session ($F(1,32)=86.82$, $p<.001$), $F(1,32)=5.62$, $p=.02$, indicating a degree of habituation. There was also a significant Group effect ($F(1,32)=32.03$, $p<.001$). Pairwise contrasts indicated that the High-BI group froze more than the other groups ($ps<.03$) and the Middle-BI group froze more than the Low-BI group ($p<.001$). That is, both the High- and Low-BI groups showed elevated freezing relative to the Middle group. These differences were particularly pronounced during the encounter with the intruder ($F(1,32)=7.79$, $p=.002$); specifically, the three groups significantly differed in freezing when the intruder was present ($ps<.003$); whereas, the Middle-BI group did not differ from the High- ($p=.38$) or Low-BI groups ($p=.07$) when the intruder was absent.

Notably, when directly compared with the Low-BI group, the High-BI group showed an 18-fold difference in freezing when the intruder was present ($p<.001$) as well as a 13-fold difference in freezing when the intruder was absent ($p=.008$) (**see Table S1**). These results indicate that although the BI phenotype is

most strongly expressed in response to overt threat, it also manifests in response to the diffusely threatening test cage. ***Following the second screening session, only the two extreme BI groups were further assessed.***

The High-BI Group Shows Elevated Freezing in Response to the Live Snake and Perceptually-Similar Control Stimuli

During each trial of the snake-anxiety assessment, freezing behavior was quantified by an experienced observer, similar to the procedures used for initial phenotyping (**Table S2**). Analyses revealed a significant effect of Stimulus ($F(3,63)=6.54$, $p=.01$) as well as a significant linear effect of Stimulus (Live Snake > Artificial Snake > Tape > Nothing, $F(1,21)=7.63$, $p=.01$). The GLM also demonstrated that the High-BI group showed a trend to freeze more than the Low-BI group ($F(1,21)=4.35$, $p=.053$), although this effect was tempered by a near-significant Group × Stimulus interaction ($F(3,63)=3.59$, $p=.06$). Follow-up tests indicated that the High-BI group titrated freezing to the degree of threat or perceptual similarity to the live snake (Live Snake > Artificial Snake > Tape > Nothing, $F(1,21)=5.44$, $p=.04$; all pairwise differences were in the predicted direction and significant [$ps<.05$] except for the live vs. artificial snake difference [$p=.07$]). In contrast, the Low-BI group showed uniformly low levels of freezing across stimuli (pairwise $ps>.22$). Across the two extreme groups, individuals who froze more in the presence of the live snake also showed increased freezing in response to the human intruder's profile during the initial screening sessions more than two years earlier, $r=.43$, $p=.04$. Not surprisingly, individuals who froze more in the presence of the live snake also tended to commit more non-responses, $\rho=.47$, $p=.02$.

Exploratory Analyses of Response Time (RT) During the Snake Anxiety Assessment

Exploratory analyses of RT in the subset of subjects with complete RT data for every condition ($N=15$; High-BI: $n=5/11$; Low-BI: $n=10/12$) were broadly consistent with prior work using unselected samples of laboratory-raised monkeys[8, 21, 22]. There was a significant effect of Stimulus ($F(3,39)=7.17$, $p=.001$ and a significant linear effect of Stimulus on response latency (Live Snake > Artificial Snake > Tape > Nothing), $F(1,13)=17.91$, $p=.001$. The live snake was associated with slower responses than the roll of tape and nothing ($ps<.03$), but not the artificial snake ($p=.48$). Neither the Group nor the Group × Stimulus effects was significant, $ps>.08$.

Supplementary Table S1. *Freezing duration during the two initial 10-min phenotyping sessions.*

	High-BI[a]		Mid-BI[b]		Low-BI[c]		All Individuals[d]	
Total Freezing (seconds)	*M*	*SD*	*M*	*SD*	*M*	*SD*	*M*	*SD*
Alone-1	19.3	35.5	15.1	19.0	1.5	2.6	10.7	18.5
Alone-2	37.7	66.4	8.0	10.0	2.9	5.2	17.4	36.3
NEC-1	401.7	64.3	141.9	37.5	28.1	20.1	187.5	133.5
NEC-2	328.9	56.2	126.0	39.3	12.3	14.1	135.6	115.0

[a] N=11. [b] N=12. [c] N=12. [d] N=109. [e] Hypothesis testing was performed using $\log_{10}$-transformed mean freezing duration.

Supplementary Table S2. *Freezing duration during the 30-min experimental sessions.*

	High-BI[a]		Low-BI[b]	
Total Freezing (seconds)	*M*	*SD*	*M*	*SD*
Alone	150.0	165.7	30.8	29.1
Intruder	443.5	414.0	54.7	58.8
Alone-Following-Alone	113.6	207.8	30.4	50.9
Alone-Following-Intruder	211.8	201.5	24.8	29.9

[a] N=11. [b] N=12. [c] Hypothesis testing was performed using $\log_{10}$-transformed mean freezing duration (across six successive 5-min epochs).

Supplementary Table S3. *Descriptive statistics for clusters identified by the Group × Condition interaction*

				Local Maxima (millimeters from AC)		
Cluster	Volume (mm^3)	Includes	t^a	*x*	*y*	*z*
R BST	43.2[b]	BST, EGP, IC, AC	-4.93	5.625	0.000	2.500
R Parietal	35.4[c]	Area PG	4.85	18.750	-21.875	18.750

[a] Regression controlling for nuisance variation in mean-centered gray matter probability.
[b] Cluster lies inside the *a priori* extended amygdala ROI and is significant ($p<.05$, small-volume corrected).
[c] Cluster lies outside the *a priori* extended amygdala ROI and is not significant using a whole-brain threshold.
Abbreviations—AC: anterior commissure; **BST:** bed nucleus of the stria terminalis; **EGP:** external blobus pallidus; **IC:** internal capsule; **L:** Left; **NAcc:** nucleus accumbens; **R:** Right. Clusters were sorted from anterior to posterior and labeled using the Paxinos atlas[24], freely available at http://scalablebrainatlas.incf.org/main/coronal3d.php?template=PHT00&.

Supplementary Table S4. *Descriptive statistics for clusters showing significantly more activity for the High-BI compared to the Low-BI group following the intruder encounter*

				Local Maxima (millimeters from AC)		
Cluster	Volume (mm^3)	Includes	t^a	*x*	*y*	*z*
L dlPFC	16.6[c]	Areas 46, 8AD	-3.41	-14.375	6.875	12.500
L BST	33.2[b]	BST, EGP, IC, AC	4.69	-4.375	-0.625	2.500
R BST	46.4[b]	BST, EGP, IC, AC	5.10	4.375	0.000	0.625
R Frontal	53.2[c]	Areas 3, 6V	3.69	21.875	-1.875	13.125
			3.68	26.875	-1.875	8.750
L Hypoth.	31.0[c]		5.13	-2.500	-1.875	-4.375
R Hypoth.	53.2[c]		3.22	28.750	-2.500	5.000
R Insula	63.0[c]	AI, DI, Ipro, PaAR	4.35	21.250	-5.000	-4.375
L Frontal	39.1[c]	Areas 2, 3	3.64	-26.875	-5.000	6.875
			3.37	-23.125	-8.125	10.625
Bi. Brainstem	35.4[c]	3N, red nucleus	3.91	0.000	-11.250	-15.625
R Cerebellar peduncle	49.3[c]		-4.12	15.000	-18.750	-15.625
R ITS	33.4[c]	Area TF	4.14	18.750	-12.500	-6.250
L Visual	195.8[c]	V1, V2	-4.07	-10.625	-29.375	1.875
R Visual	325.7[d]	V1, V2	-3.78	7.500	-37.500	3.125
			-3.64	16.250	-38.125	2.500

[a] Regression controlling for nuisance variation in mean-centered gray matter probability.
[b] Cluster lies inside the *a priori* extended amygdala ROI and is significant ($p<.05$, small-volume corrected).
[c] Cluster lies outside the *a priori* extended amygdala ROI and is not significant using a whole-brain threshold ($p>.05$, whole-brain corrected).
[d] Cluster lies outside the *a priori* extended amygdala ROI and is significant using a whole-brain threshold ($p<.05$, whole-brain corrected).
Abbreviations—3N: oculomotor nucleus; **AC:** anterior commissure; **AI:** agranular insula; **Bi:** bilateral; **BST:** bed nucleus of the stria terminalis; **DI:** dysgranular insula; **dlPFC:** dorsolateral prefrontal cortex; **EGP:** external globus pallidus; **Hypoth:** hypothalamus; **IC:** internal capsule; **Ipro:** insular proisocortex; **ITS:** inferior temporal sulcus; **L:** Left; **PaAR:** posterior para-auditory cortex; **R:** Right. Clusters were sorted from anterior to posterior and labeled using the Paxinos atlas[24], freely available at http://scalablebrainatlas.incf.org/main/coronal3d.php?template=PHT00&.

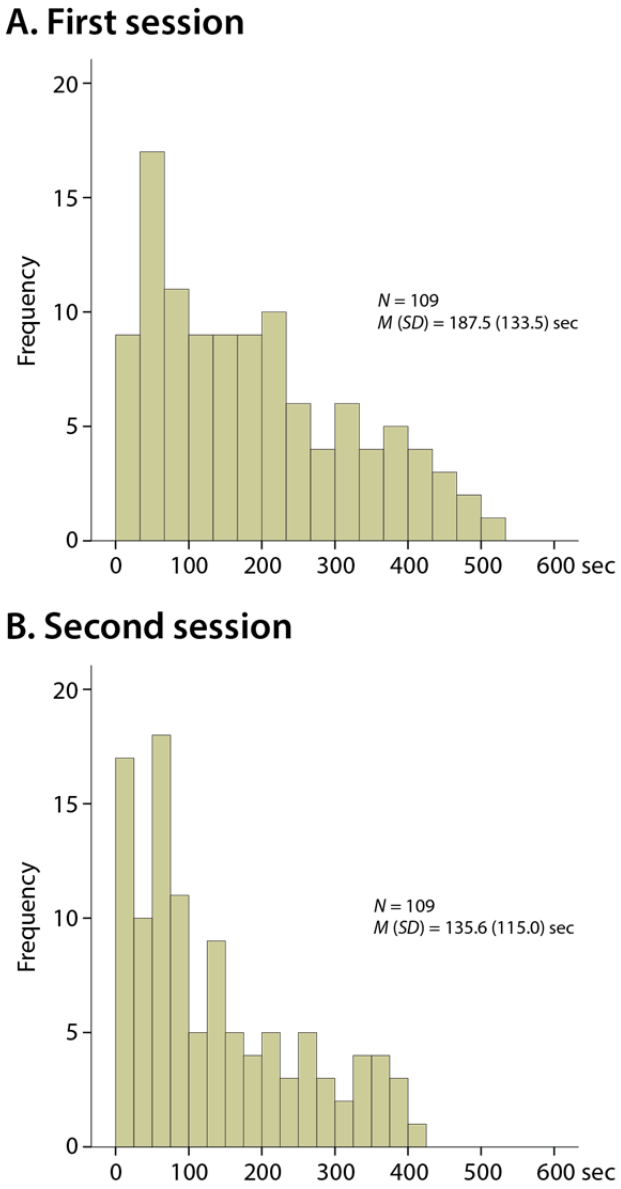

Supplementary Figure S1. Individual differences in intruder-elicited freezing during the initial phenotyping sessions. Individual differences in freezing elicited by a unfamiliar human intruder's profile (600 sec) were assessed on two occasions, one week apart, using the 'No Eye Contact' condition of the Human Intruder Paradigm[7, 10]. Individual differences in intruder-elicited freezing were continuously distributed without obvious gaps or discontinuities, consistent with prior work by our group[34]. ***A. Histogram for the first session. B. Histogram for the second session.***

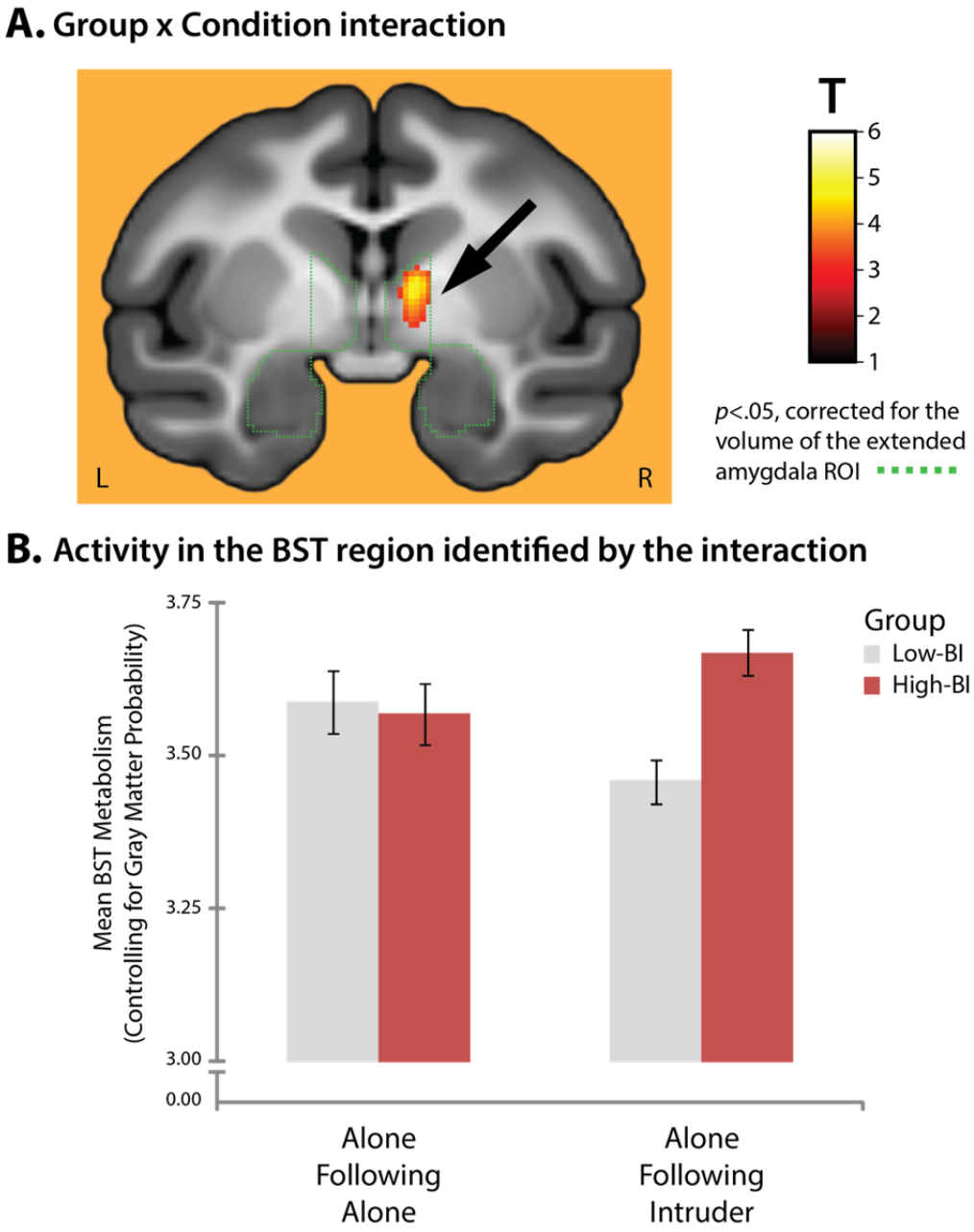

Supplementary Figure S2. The High-BI group shows elevated metabolic activity in the region of the BST following the intruder encounter. The *a priori* extended amygdala ROI is indicated by the dashed green line. The imaging paradigm is depicted in Figure 1d. ***A. Regions showing a significant Group × Condition interaction.*** The cluster in the region of the BST is indicated by the black arrow (p<.05, small-volume corrected). ***B. Activity in the BST region identified by the interaction.*** Figure shows mean activity from the cluster depicted in panel A controlling for nuisance variance in mean-centered gray matter probability. Error bars depict SE.

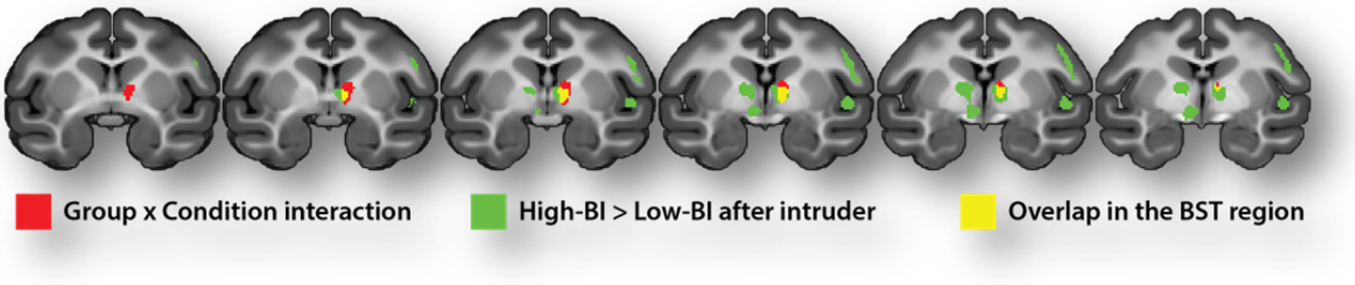

Supplementary Figure S3. The High-BI group shows elevated metabolic activity in the region of the BST following the intruder encounter. Sequential coronal slices running from most rostral (left) to most caudal (right). BST clusters are centered in the region demarcated by the caudate (dorsal), midline/third ventricle (mesial), and external globus pallidus (ventral and lateral). The region of overlap (depicted in yellow to maximize visual contrast) corresponds to the region depicted in purple in Figures 3c and 3d in the main report.

SUPPLEMENTARY REFERENCES

1. Kalin NH, Shelton SE, Fox AS, Rogers J, Oakes TR, Davidson RJ. The serotonin transporter genotype is associated with intermediate brain phenotypes that depend on the context of eliciting stressor. *Mol Psychiatry* 2008; **13:** 1021-1027.

2. Fox AS, Shelton SE, Oakes TR, Davidson RJ, Kalin NH. Trait-like brain activity during adolescence predicts anxious temperament in primates. *PLoS ONE* 2008; **3:** e2570.

3. Jahn AL, Fox AS, Abercrombie HC, Shelton SE, Oakes TR, Davidson RJ *et al.* Subgenual prefrontal cortex activity predicts individual differences in hypothalamic-pituitary-adrenal activity across different contexts. *Biol Psychiatry* 2010; **67:** 175-181.

4. Oler JA, Fox AS, Shelton SE, Christian BT, Murali D, Oakes TR *et al.* Serotonin transporter availability in the amygdala and bed nucleus of the stria terminalis predicts anxious temperament and brain glucose metabolic activity. *J Neurosci* 2009; **29:** 9961-9966.

5. Rawlins RG, Kessler MJ. Demography of th free-ranging Cayo Santiago macaques (1976-1983). In: Rawlins RG, Kessler MJ (eds). *The Cayo Santiago macaques. History, behavior, and biology*. SUNY Press: Albany, NY, 1986, pp 47-72.

6. Fox AS, Kalin NH. A translational neuroscience approach to understanding the development of social anxiety disorder and its pathophysiology. *Am J Psychiatry* 2014; **171:** 1162-1173.

7. Kalin NH, Shelton SE. Defensive behaviors in infant rhesus monkeys: environmental cues and neurochemical regulation. *Science* 1989; **243:** 1718-1721.

8. Kalin NH, Shelton SE, Davidson RJ. The role of the central nucleus of the amygdala in mediating fear and anxiety in the primate. *J Neurosci* 2004; **24:** 5506-5515.

9. Kalin NH, Shelton SE, Fox AS, Oakes TR, Davidson RJ. Brain regions associated with the expression and contextual regulation of anxiety in primates. *Biol Psychiatry* 2005; **58:** 796-804.

10. Oler JA, Fox AS, Shackman AJ, Kalin NH. The central nucleus of the amygdala is a critical substrate for individual differences in anxiety. In: Amaral DG, Adolphs R (eds). *Living without an amygdala*. Guilford: NY, 2016.

11. Kalin NH. The neurobiology of fear. *Sci Am* 1993; **268:** 94-101.

12. Volbrecht MM, Goldsmith HH. Early temperamental and family predictors of shyness and anxiety. *Dev Psychol* 2010; **46:** 1192-1205.

13. Kagan J, Reznick JS, Snidman N. Biological bases of childhood shyness. *Science* 1988; **240:** 167-171.

14. Hirshfeld-Becker DR, Micco J, Henin A, Bloomfield A, Biederman J, Rosenbaum J. Behavioral inhibition. *Depress Anxiety* 2008; **25:** 357-367.

15. Chronis-Tuscano A, Degnan KA, Pine DS, Perez-Edgar K, Henderson HA, Diaz Y *et al.* Stable early maternal report of behavioral inhibition predicts lifetime social anxiety disorder in adolescence. *J Am Acad Child Adolesc Psychiatry* 2009; **48:** 928-935.

16. Blackford JU, Clauss JA. Dr. Blackford and Ms. Clauss reply. *J Am Acad Child Adolesc Psychiatry* 2013; **52:** 319-320.

17. Clauss JA, Blackford JU. Behavioral inhibition and risk for developing social anxiety disorder: a meta-analytic study. *J Am Acad Child Adolesc Psychiatry* 2012; **51:** 1066-1075

18. Essex MJ, Klein MH, Slattery MJ, Goldsmith HH, Kalin NH. Early risk factors and developmental pathways to chronic high inhibition and social anxiety disorder in adolescence. *Am J Psychiatry* 2010; **167:** 40-46.

19. Brooker RJ, Buss KA, Lemery-Chalfant K, Aksan N, J. DR, Goldsmith HH. The development of stranger fear in infancy and toddlerhood: Normative development, individual differences, antecedents, and outcomes. *Developmental Science in press*.

20. Preacher KJ, Rucker DD, MacCallum RC, Nicewander WA. Use of the extreme groups approach: A critical reexamination and new recommendations. *Psychol Methods* 2005; **10:** 178-192.

21. Kalin NH, Shelton SE, Davidson RJ, Kelley AE. The primate amygdala mediates acute fear but not the behavioral and physiological components of anxious temperament. *J Neurosci* 2001; **21:** 2067-2074.

22. Nelson EE, Shelton SE, Kalin NH. Individual differences in the responses of naive rhesus monkeys to snakes. *Emotion* 2003; **3:** 3-11.

23. Tai YC, Chatziioannou A, Siegel S, Young J, Newport D, Goble RN *et al.* Performance evaluation of the microPET P4: a PET system dedicated to animal imaging. *Phys Med Biol* 2001; **46:** 1845-1862.

24. Paxinos G, Huang X, Petrides M, Toga A. *The rhesus monkey brain in stereotaxic coordinates*. 2nd edn. Academic Press: San Diego, 2009.

25. Oakes TR, Fox AS, Johnstone T, Chung MK, Kalin N, Davidson RJ. Integrating VBM into the general linear model with voxelwise anatomical covariates. *Neuroimage* 2007; **34:** 500-508.

26. Christopoulos GI, Tobler PN, Bossaerts P, Dolan RJ, Schultz W. Neural correlates of value, risk, and risk aversion contributing to decision making under risk. *J Neurosci* 2009; **29**(40)**:** 12574-12583.

27. Nichols T, Brett M, Andersson J, Wager T, Poline JB. Valid conjunction inference with the minimum statistic. *Neuroimage* 2005; **25:** 653-660.

28. Watson D, Walker LM. The long-term stability and predictive validity of trait measures of affect. *J Pers Soc Psychol* 1996; **70**(3)**:** 567-577.

29. Chmielewski M, Watson D. What is being assessed and why it matters: the impact of transient error on trait research. *J Pers Soc Psychol* 2009; **97:** 186-202.

30. Kalin NH, Shelton S. The regulation of defensive behaviors in rhesus monkeys. In: Davidson RJ (ed). *Anxiety, depression, and emotion*. Oxford University Press: NY, 2000, pp 50-68.

31. Lee FS, Heimer H, Giedd JN, Lein ES, Sestan N, Weinberger DR *et al.* Mental health. Adolescent mental health--opportunity and obligation. *Science* 2014; **346:** 547-549.

32. Kriegeskorte N, Simmons WK, Bellgowan PS, Baker CI. Circular analysis in systems neuroscience: the dangers of double dipping. *Nat Neurosci* 2009; **12:** 535-540.

33. Kriegeskorte N, Lindquist MA, Nichols TE, Poldrack RA, Vul E. Everything you never wanted to know about circular analysis, but were afraid to ask. *J Cereb Blood Flow Metab* 2010; **30:** 1551-1557.

34. Shackman AJ, Fox AS, Oler JA, Shelton SE, Davidson RJ, Kalin NH. Neural mechanisms underlying heterogeneity in the presentation of anxious temperament. *Proc Natl Acad Sci U S A* 2013; **110:** 6145-6150.